

# UC San Diego

## UC San Diego Previously Published Works

### Title

Deletion or Inhibition of the Oxygen Sensor PHD1 Protects against Ischemic Stroke via Reprogramming of Neuronal Metabolism

### Permalink

<https://escholarship.org/uc/item/4rz5d7c1>

### Journal

Cell Metabolism, 23(2)

### ISSN

1550-4131

### Authors

Quaegebeur, Annelies  
Segura, Inmaculada  
Schmieder, Roberta  
[et al.](#)

### Publication Date

2016-02-01

### DOI

10.1016/j.cmet.2015.12.007

Peer reviewed



Published in final edited form as:

*Cell Metab.* 2016 February 9; 23(2): 280–291. doi:10.1016/j.cmet.2015.12.007.

## DELETION OR INHIBITION OF THE OXYGEN SENSOR PHD1 PROTECTS AGAINST ISCHEMIC STROKE VIA REPROGRAMMING OF NEURONAL METABOLISM

Annelies Quaegebeur<sup>1,2</sup>, Inmaculada Segura<sup>1,2</sup>, Roberta Schmieder<sup>3,4</sup>, Dries Verdegem<sup>1,2</sup>, Ilaria Decimo<sup>1,2</sup>, Francesco Bifari<sup>1,2</sup>, Tom Dresselaers<sup>5</sup>, Guy Eelen<sup>1,2</sup>, Debapriya Ghosh<sup>6</sup>, Sandra Schoors<sup>1,2</sup>, Sudha Rani Janaki Raman<sup>3,4</sup>, Bert Cruys<sup>1,2</sup>, Kristof Govaerts<sup>5</sup>, Carla De Legher<sup>1,2</sup>, Ann Bouché<sup>1,2</sup>, Luc Schoonjans<sup>1,2</sup>, Matt S. Ramer<sup>1,2,7</sup>, Gene Hung<sup>8</sup>, Goele Bossaert<sup>9</sup>, Don W. Cleveland<sup>10</sup>, Uwe Himmelreich<sup>5</sup>, Thomas Voets<sup>6</sup>, Robin Lemmens<sup>11,12,13</sup>, C. Frank Bennett<sup>8</sup>, Wim Robberecht<sup>11,12,13</sup>, Katrien De Bock<sup>1,2,\*</sup>, Mieke Dewerchin<sup>1,2</sup>, Sarah-Maria Fendt<sup>3,4</sup>, Bart Ghesquière<sup>14</sup>, and Peter Carmeliet<sup>1,2</sup>

<sup>1</sup>Laboratory of Angiogenesis and Neurovascular link, Department of Oncology, University of Leuven, Leuven, Belgium

<sup>2</sup>Laboratory of Angiogenesis and Neurovascular link, Vesalius Research Center, VIB, Leuven, Belgium

<sup>3</sup>Laboratory of Cellular Metabolism and Metabolic Regulation, Department of Oncology, University of Leuven, Leuven, Belgium

<sup>4</sup>Laboratory of Cellular Metabolism and Metabolic Regulation, Vesalius Research Center, VIB, Leuven, Belgium

<sup>5</sup>Biomedical MRI/Mosaic, Department of Imaging and Pathology, University of Leuven, Leuven, Belgium

<sup>6</sup>Laboratory of Ion Channel Research and TRP channel research platform Leuven, Department of Cellular and Molecular Medicine, University of Leuven, Leuven, Belgium

<sup>7</sup>International Collaboration on Repair Discoveries, the University of British Columbia, Vancouver, Canada

<sup>8</sup>Isis Pharmaceuticals, Carlsbad, CA

Editorial correspondence: P. Carmeliet, M.D., Ph.D., Laboratory of Angiogenesis and Neurovascular link, Vesalius Research Center, VIB, KU Leuven, Campus Gasthuisberg O&N4, Herestraat 49 - 912, B-3000, Leuven, Belgium, tel: 32-16-37.32.02; fax: 32-16-37.25.85; ; Email: peter.carmeliet@vib-kuleuven.be

\*current address: Department Health Sciences and Technology, Laboratory of Exercise and Health, Swiss Federal Institute of Technology (ETH) Zurich, Zurich, Switzerland.

### Authorship contributions

PC conceptualized and AQ conducted the project. AQ, IS, RS, ID, FB, TD, DB, GE, BC, SRJR, MSR performed experiments and analyzed the data. DD and KG analyzed data. AB and CDL performed experiments. AQ, IS, ID, FB, SS, RL, RS, SMF, TV, UH, KDB and PC designed experiments. DWC, CFB and GH provided the design of ASOs and advice on the ASO-experiments. IS, ID, FB, SMF, KDB, WR, MD, RL and LS provided scientific suggestions, and contributed to the manuscript review. AQ, IS and PC wrote the manuscript. All authors edited the paper.

### Conflict-of-interest disclosure

G. Hung and C.F. Bennett are employees of Isis Pharmaceuticals Inc. and could materially benefit if a therapeutic product for treatment of ischemic stroke results from this work.

<sup>9</sup>Leuven Statistics Research Centre (LStat), University of Leuven, Leuven, Belgium

<sup>10</sup>Ludwig Institute for Cancer Research, Department of Medicine and Neuroscience, University of California, San Diego, La Jolla, CA 92093, USA

<sup>11</sup>Laboratory of Neurobiology, Vesalius Research Center, VIB, Leuven, Belgium

<sup>12</sup>Experimental Neurology (Department of Neurosciences) and Leuven Research Institute for Neuroscience and Disease (LIND), University of Leuven, Leuven, Belgium

<sup>13</sup>Neurology, University Hospitals Leuven, Leuven, Belgium

<sup>14</sup>Metabolomics Expertise Center, Vesalius Research Center, VIB, Leuven, Belgium

## Summary

The oxygen-sensing prolyl hydroxylase domain proteins (PHDs) regulate cellular metabolism, but their role in neuronal metabolism during stroke is unknown. Here we report that PHD1 deficiency provides neuroprotection in a murine model of permanent brain ischemia. This was not due to an increased collateral vessel network, nor to enhanced neurotrophin expression. Instead, PHD1<sup>-/-</sup> neurons were protected against oxygen-nutrient deprivation by reprogramming glucose metabolism. Indeed, PHD1<sup>-/-</sup> neurons enhanced glucose flux through the oxidative pentose phosphate pathway by diverting glucose from glycolysis. As a result, PHD1<sup>-/-</sup> neurons increased their redox buffering capacity to scavenge oxygen radicals in ischemia. Intracerebroventricular injection of PHD1-antisense oligonucleotides reduced the cerebral infarct size and neurological deficits following stroke. These data identify PHD1 as a novel regulator of neuronal metabolism and a potential therapeutic target in ischemic stroke.

## Introduction

The brain is the largest consumer of oxygen and glucose in the human body. It is well established that this organ relies primarily on oxidative glucose metabolism for the production of energy (Howarth et al., 2012; Mergenthaler et al., 2013). However, in contrast to the knowledge on how cancer cells and some other non-transformed cell types (immune cells, endothelial cells, etc.) alter their metabolism in disease (DeBerardinis and Cheng, 2010; Ghesquiere et al., 2014; Schulze and Harris, 2012; Vander Heiden et al., 2009), it remains poorly understood how neurons adapt their metabolism upon ischemic neuronal injury. In fact, there is even ongoing debate about the precise metabolism of neurons in baseline conditions (Belanger et al., 2011; Jolivet et al., 2010; Mangia et al., 2011). Apart from some studies (Cui et al., 2006; Fang et al., 2014; Knight et al., 2014; Morais et al., 2014; Rodriguez-Rodriguez et al., 2013; Tufi et al., 2014), it remains largely unknown if neuronal metabolism is a target to promote neuroprotection.

This is nonetheless an important question, since ischemic stroke, resulting from acute arterial occlusion, is currently the fourth leading cause of death and the most common reason of severe disability, for which there is a large unmet medical need for efficient therapies. A main target of such therapies is the ischemic penumbra, a region surrounding a core of necrotic tissue. It suffers only moderate blood flow reduction, and remains viable during a limited period of time before a cascade of deleterious events threatens the energy

and redox homeostasis, ultimately causing ischemic neuronal death (Lo et al., 2003; Moskowitz et al., 2010). This salvageable tissue is the target of reperfusion and neuroprotective strategies (Moskowitz et al., 2010). Nonetheless, despite progress in preclinical studies, there are no clinically approved neuroprotective treatments.

Prolyl hydroxylase domain proteins (PHD1-3) are master regulators of the response to hypoxia (Quaegebeur and Carmeliet, 2010; Semenza, 2011). Since their hydroxylation of target proteins is oxygen-dependent, PHDs act as oxygen sensors. The transcription factors hypoxia-inducible factor (HIF)-1 $\alpha$  and HIF-2 $\alpha$  are the best characterized PHD targets, yet many other targets continue to be identified (Wong et al., 2013). When oxygen is present, PHD-mediated hydroxylation targets proteins for proteasomal degradation. Thus, when oxygen levels drop and PHDs lose their activity, HIFs and other target proteins accumulate (Quaegebeur and Carmeliet, 2010; Semenza, 2011).

Surprisingly little is known about the functions of the PHDs in the brain. Moreover, PHDs have been implicated in instructing various metabolic adaptations, but primarily in cell types other than neurons. In general, through stabilization of HIFs, PHD inhibition induces a shift from oxidative to anaerobic metabolism, thereby enhancing glycolysis at the expense of glucose oxidation (Aragones et al., 2009). For instance, loss of PHD1 makes the muscle and liver ischemia-tolerant by shifting mitochondrial metabolism towards anaerobic glycolysis (Aragones et al., 2008; Schneider et al., 2009). However, it remains unknown if PHDs control metabolism of neurons in a similar manner, and whether HIFs are their primary target in this process. In this study, we examined the role of the oxygen sensor PHD1 in brain ischemia after stroke induction, and focused on its possible role in controlling neuronal metabolism in this process.

Our results show that deletion of PHD1 largely prevented brain ischemic injury after stroke induction. In contrast to the metabolic phenotype in PHD1<sup>-/-</sup> muscle (Aragones et al., 2008), PHD1<sup>-/-</sup> neurons shunted more glucose into the anti-oxidant pentose phosphate pathway (PPP), while reducing glycolytic flux. This enabled PHD1<sup>-/-</sup> neurons to maintain redox homeostasis during ischemic events. Of therapeutic importance, silencing of PHD1 by intracerebroventricular delivery of antisense oligonucleotides protected against brain ischemia. These findings not only identify a novel therapeutic target for ischemic stroke but also provide novel insights into the link between oxygen sensors, metabolism and neuroprotection.

## Results

### PHD1<sup>-/-</sup> mice are protected against permanent brain ischemia

To assess whether PHDs play a role in brain ischemia, we performed a permanent middle cerebral artery occlusion (pMCAO) in previously generated PHD1 deficient (PHD1<sup>-/-</sup>) and PHD3 deficient (PHD3<sup>-/-</sup>) mice. Since homozygous PHD2 deficiency is embryonically lethal (Takeda et al., 2006), we used PHD2<sup>NKO</sup> mice, i.e. neural specific PHD2 deficient mice, obtained by intercrossing Nestin-Cre mice (Tronche et al., 1999) with PHD2<sup>lox/lox</sup> mice (Mazzone et al., 2009). To assess the cerebral infarct area, we stained brain slices with the vital dye 2,3,5-triphenyltetrazolium chloride (TTC) at 24 hours post-pMCAO when

lesion size is maximal (Kuraoka et al., 2009). Brain ischemia was substantially attenuated in PHD1<sup>-/-</sup> mice with an approximately 70% reduction in ischemic lesion size when compared to wild type (WT) mice (Figure 1A–C), whereas stroke size was not affected in PHD2<sup>NKO</sup> and PHD3<sup>-/-</sup> mice (Figure 1D–I). Strain-dependent differences in stroke size have been reported in the literature (Barone et al., 1993; Connolly et al., 1996; Fujii et al., 1997; Majid et al., 2000). However, PHD1<sup>-/-</sup> mice on a 129S6 background (Figure S1A–C) were protected to a similar extent against ischemic brain injury as C57Bl/6N mice (Figure 1A–C).

To test whether the smaller infarct size in PHD1<sup>-/-</sup> mice improved functional outcome, we used the adhesive tape removal test (Bouet et al., 2009). Following pMCAO, WT mice showed a delay in time necessary to sense and remove the tape, indicative of an impaired sensorimotor coordination. In line with a smaller infarct lesion, post-stroke functional impairment was nearly completely prevented in PHD1<sup>-/-</sup> mice (Figure 1J,K).

To exclude that constitutive PHD1 deficiency elicited compensatory changes in other oxygen sensors, we measured transcript levels of *Phd2* and *Phd3*. These were however not augmented in PHD1<sup>-/-</sup> brains (mRNA copies/10<sup>3</sup> copies *HPRT*: 13.9 ± 0.4 in WT and 14.7 ± 0.7 in PHD1<sup>-/-</sup> for *Phd2*; 2.2 ± 0.11 in WT and 2.3 ± 0.05 in PHD1<sup>-/-</sup> for *Phd3*; n = 4; p = NS).

### PHD1 deficiency does not cause vascular changes in the brain

We then investigated the mechanism via which PHD1 deficiency governed ischemic protection in the brain. We first focused on the brain vasculature, as PHDs regulate angiogenesis, collateral vessel growth and organ perfusion (Quaegebeur and Carmeliet, 2010). Also, stroke size has been inversely associated with the extent of collateral flow in mice and patients (Shuaib et al., 2011; Zhang et al., 2010). In baseline conditions, perfusion with FITC-conjugated dextran showed a similar area of perfused vessels in the cortical area of (non-stroked) WT *versus* PHD1<sup>-/-</sup> brains (Figure 2A–C). In addition, we performed three-dimensional corrosion casting of the brain vasculature after infusion of a resin to image the perfused pial collateral vessels, a main contributor to collateral flow in the stroke area in experimental pMCAO (Zhang et al., 2010). This analysis showed a similar number of pial collaterals in WT and PHD1<sup>-/-</sup> brains (Figure 2D–F). Consistent with these data, immunostaining for  $\alpha$ -smooth muscle actin ( $\alpha$ -SMA), visualizing the conducting arterioles and arteries, did not reveal genotypic differences (Figure S2A–C). These data indicate that PHD1 deficiency did not alter structural features of the brain vasculature. Circulating erythropoietin and hematocrit levels, determining the oxygen carrying potential of the blood that might affect the infarct size by improving tissue oxygenation (Sakanaka et al., 1998; Siren et al., 2001), were unaltered in PHD1<sup>-/-</sup> mice (Aragones et al., 2008).

Since preconditioning has been described to enhance cerebral perfusion after stroke (Gidday, 2006), we assessed whether vessel perfusion was improved in PHD1<sup>-/-</sup> mice following pMCAO, even despite similar baseline vessel parameters. First, we calculated the fraction of perfused vessels in the stroke area *versus* contralateral cortex, by identifying vessels with isolectin-B4 staining and perfusion with FITC-dextran injection at two hours after pMCAO. This analysis did not show a difference in the fraction of perfused vessels in PHD1<sup>-/-</sup> mice in the stroke area or contralateral side (Figure 2G–K). Next, we used *in vivo* magnetic

resonance (MR) imaging to assess the perfusion deficit (defined as the area where the cerebral blood flow (CBF) was lower than 80% of the CBF in the contralateral cortex) and lesion size (volumes of increased T2 values) using arterial spin labeling (ASL). Consistent with a smaller infarct size on vital dye staining, T2-weighted MR images showed a smaller lesion volume in PHD1<sup>-/-</sup> mice at 24 hours after arterial occlusion (Figure 2L,M). The perfusion deficit was however similar between the two genotypes, both at 2 and 24 hours following arterial ligation (Figure 2N).

### PHD1 deficiency protects against oxygen-nutrient deprivation *in vitro*

Given the lack of prominent vascular changes in PHD1<sup>-/-</sup> brains, we hypothesized that PHD1 deficiency might confer neuroprotection by modulating intrinsic neuronal properties. We therefore assessed the effect of oxygen/glucose shortage in 7 days *in vitro* (DIV) cortical neurons by exposing WT and PHD1<sup>-/-</sup> cultures to two hours of oxygen-nutrient deprivation (*i.e.* 0.1% O<sub>2</sub> in medium lacking glucose, glutamine and pyruvate) after which they were re-exposed to ambient air and nutrient-rich medium (an established *in vitro* model of brain ischemia *in vivo* (Koh and Choi, 1987; Meloni et al., 2011)). After 24 hours, neuronal cell death, quantified by measuring LDH release in the medium, was substantially reduced in PHD1<sup>-/-</sup> neurons (Figure 2O).

We then explored whether the neuroprotection was specific for PHD1 deficiency. In accordance with the absence of induced expression of other PHD enzymes in PHD1<sup>-/-</sup> brains, the transcript and protein levels of PHD2 and PHD3 in PHD1<sup>-/-</sup> neurons did not differ from those of their WT counterparts (Figure S2D–E). Of importance, PHD2 and PHD3 silencing (by lentiviral transduction of a specific shRNA, reducing *Phd2* and *Phd3* mRNA levels by up to 80–85% and 70%, respectively) in WT neurons did not confer protection against *in vitro* oxygen-nutrient deprivation (Figure 2P), indicating a PHD1-specific effect, in accordance with the PHD1-specific protection in the pMCAO model.

To exclude the possibility that structural differences in PHD1<sup>-/-</sup> embryos or different PHD1<sup>-/-</sup> neuronal culture features contributed to this resilience against *in vitro* ischemia, we performed additional control experiments. Macroscopic inspection of embryos revealed that loss of PHD1 did not cause prominent developmental central nervous system defects. Also, Nissl staining revealed a normal brain cytoarchitecture in E14.5 PHD1<sup>-/-</sup> embryos (Figure S2F–I). In agreement, similar numbers of cortical neurons were isolated from E14.5 PHD1<sup>-/-</sup> embryos, which appeared morphologically normal (Figure S2J,K). There were also no genotypic differences in the fraction of contaminating non-neuronal cells (<2%) in the cultures, as determined by staining for the glial marker GFAP, and the oligodendrocyte markers NG2 and Olig2 (not shown).

In an initial effort to explore the underlying mechanism of the angiogenesis-independent neuroprotection, we first assessed whether PHD1 deficiency upregulated the expression of neuroprotective factors, since enhanced neurotrophin expression is known to protect against neuronal ischemia (Ferenz et al., 2012; Klumpp et al., 2006). However, we did not observe genotypic differences in the mRNA expression of neurotrophic factors and their receptors in WT and PHD1<sup>-/-</sup> neurons (Table S1).

## PHD1 deficiency reprograms glucose metabolism in neurons

Since PHD1 deficiency has previously been linked to protection against muscle ischemia via altering its glucose metabolism (Aragones et al., 2008), we explored whether PHD1 deficiency would prepare neurons for an ischemic insult by altering neuronal metabolism in baseline conditions. By reducing pyruvate entry into mitochondria, PHD1<sup>-/-</sup> muscle fibers reduce their respiration rate and, as a consequence, produce less reactive oxygen species (ROS) (Aragones et al., 2008). In addition, glycolytic flux is increased, likely as a compensation to maintain ATP levels (Aragones et al., 2008). Hence, we asked whether a similar metabolic shift contributed to ischemia tolerance in PHD1<sup>-/-</sup> neurons.

Surprisingly, however, and in sharp contrast to the metabolic phenotype of PHD1<sup>-/-</sup> muscle fibers, the glycolytic rate of PHD1<sup>-/-</sup> neurons in baseline conditions, quantified by the production of <sup>3</sup>H<sub>2</sub>O after supplementation with [5-<sup>3</sup>H]-glucose, was reduced by 25% (Figure 3A). In accordance, glucose consumption, evaluated by quantifying the difference in glucose levels in the medium over 24 hours, was also reduced in PHD1<sup>-/-</sup> neurons to a similar extent (Figure 3B). Since glucose in neurons is predominantly oxidized, producing CO<sub>2</sub> and NADH, a reducing agent used for ATP production in oxidative phosphorylation, we subsequently assessed whether the reduction in glycolysis led to reduced glucose oxidation. When measuring <sup>14</sup>CO<sub>2</sub> release after incubation with [6-<sup>14</sup>C]-glucose, we observed a similar (25%) reduction in glucose oxidation in PHD1<sup>-/-</sup> neurons in baseline conditions (Figure 3C).

## PHD1 loss maintains respiration and increases glutamine oxidation

We explored if the change in glucose oxidation was due to mitochondrial alterations. However, PCR analysis of mitochondrial (mtDNA) *versus* genomic (gDNA) DNA did not reveal a decrease in the number of mitochondria (gDNA/mtDNA ratio: 1.595 ± 0.065 in WT *versus* 1.565 ± 0.032 in PHD1<sup>-/-</sup>; n = 3; p = NS). Also, mitochondrial density, analyzed by staining for TOMM20, revealed no genotypic differences (Figure S3A–E).

Also at the functional level, PHD1<sup>-/-</sup> mitochondria behaved similarly as their WT counterparts. Indeed, the mitochondrial oxygen consumption rate (OCR), measured using the Seahorse extracellular flux analyzer, was not altered in PHD1<sup>-/-</sup> neurons (Figure 3D). Besides baseline OCR (OCR<sub>BAS</sub>), we also measured OCR coupled to ATP synthesis (OCR<sub>ATP</sub>; sensitive to oligomycin) and maximal respiration (OCR<sub>MAX</sub>; induced by the uncoupler dinitrophenol (DNP)) (Figure S3F). PHD1 deficiency did not affect these bioenergetic features of the mitochondria either (Figure 3E). These results were unexpected, since glucose oxidation was reduced in PHD1<sup>-/-</sup> neurons. We therefore sought to explain this apparent paradox in more detail.

A reduction in glucose oxidation could threaten energy homeostasis and jeopardize neuronal survival. However, given the comparable oxygen consumption rates in WT and PHD1<sup>-/-</sup> neurons, we hypothesized that as compensation, oxidation of alternative substrates would be enhanced. Previous studies indeed established that neurons oxidize not only glucose, but also lactate and glutamine, provided by neighboring cells (Mergenthaler et al., 2013). The oxidation of lactate (using [U-<sup>14</sup>C]-lactate) was unaffected in PHD1<sup>-/-</sup> neurons (pmol

lactate/h/10<sup>6</sup> cells: 10,510 ± 3,120 for WT *versus* 10,440 ± 2,660 for PHD1<sup>-/-</sup>; n = 3; p = NS). Glutamine is another energy substrate that after conversion first to glutamate and thereafter to α-ketoglutarate, enters the TCA cycle where it is subject to oxidation. Measuring <sup>14</sup>CO<sub>2</sub> release after incubation with [U-<sup>14</sup>C]-glutamine showed that glutamine oxidation was enhanced in PHD1<sup>-/-</sup> neurons by 37% (Figure 3F).

### PHD1 deficiency maintains energy homeostasis

These data suggest that the decrease in ATP production due to the reduction of glucose oxidation was compensated, at least in part, by enhanced production of ATP resulting from increased glutamine oxidation. Indeed, PHD1 deficiency did not alter the energy charge ( $([ATP] + \frac{1}{2} [ADP]) / ([ATP] + [ADP] + [AMP])$ ): 0.947 ± 0.005 for WT *versus* 0.942 ± 0.005 for PHD1<sup>-/-</sup>; n = 6; p = NS) or the individual values of ATP, ADP and AMP (Figure S3G). We also evaluated dendritic branching of WT and PHD1<sup>-/-</sup> neurons as an indirect, more functional read-out of mitochondrial ATP production. Indeed, dendrite morphogenesis relies on mitochondrial ATP production, and in conditions of compromised mitochondrial ATP production, dendrite branching is impaired (Oruganty-Das et al., 2012). Sholl analysis revealed however no genotypic differences in dendrite branching (Figure S3H–J).

In conditions of reduced ATP production, a cell can maintain its energy charge by lowering ATP consumption, for instance by reducing its energy demands. To exclude that the constitutive lack of PHD1 induced chronic compensatory responses preventing energy stress, we analyzed the effect of acute PHD1 silencing, as this minimizes the chance for the development of more time-requiring compensatory responses. We treated WT cultures with anti-PHD1 directed anti-sense oligonucleotides (ASOs; see below) resulting in 85 ± 7% knockdown of PHD1 mRNA levels after 48 hours. With this treatment as well, no effect on the energy charge was observed (0.956 ± 0.003 and 0.967 ± 0.004 for control *versus* 0.953 ± 0.003 and 0.968 ± 0.003 for PHD1-ASO treated neurons after 24 and 48 hours, respectively). Thus, also acute inhibition of PHD1 did not cause energetic failure. Taken together, we could not detect obvious signs of energy distress in PHD1<sup>-/-</sup> neurons.

To further exclude the possibility that PHD1<sup>-/-</sup> neurons maintained energy homeostasis by reducing their energy demands, we evaluated processes in neurons that contribute most to their energy expenditure. In neurons, maintenance of the membrane potential and synaptic activity are the main consumers of energy (Harris et al., 2012) and rely on the ATP-consuming Na<sup>+</sup>/K<sup>+</sup> pump. In order to compare its activity, we measured intracellular Na<sup>+</sup> levels. In baseline, no differences in Na<sup>+</sup> concentration could be observed between WT and PHD1<sup>-/-</sup> neurons (Figure S3K). Next, neurons were exposed to K<sup>+</sup>-free buffer, which increases intracellular Na<sup>+</sup> levels by reducing the Na<sup>+</sup>/K<sup>+</sup> pump activity. Re-exposing neurons to K<sup>+</sup>-containing buffer allowed membrane repolarization at the expense of ATP hydrolysis by the Na<sup>+</sup>/K<sup>+</sup> pump. This analysis revealed no differences in the increase of intracellular Na<sup>+</sup> levels as well as the time needed for normalization of the intracellular Na<sup>+</sup> levels, reflecting a similarly functioning antiporter pumping activity of the Na<sup>+</sup>/K<sup>+</sup> ATPase, and hence ATP consumption coupled to this key neuronal function (Figure S3L–O). Moreover, we also evaluated other processes that importantly contribute to the energy

demand in neurons, such as RNA and protein synthesis, but observed that PHD1-loss did not affect these processes (Figure S3P–U).

Overall, in contrast to the metabolic phenotype of PHD1<sup>-/-</sup> muscle, PHD1<sup>-/-</sup> neurons did not show a shift from oxidative to anaerobic metabolism, yet maintained their oxidative mitochondrial metabolism and energy homeostasis, and even lowered glycolytic flux. Notably, gene expression analysis could not link the reduced glycolysis to transcriptional changes in the expression of key glycolytic genes (Table S2).

### PHD1<sup>-/-</sup> neurons enhance the flux through the oxPPP

The above observations indicated that PHD1 deficiency regulated neuronal cell metabolism, but did not provide an explanation as to why PHD1<sup>-/-</sup> neurons were protected against ischemia. Previous work documented that glycolytic flux in neurons is kept at a low rate to enable sufficient flux of glucose into the oxidative pentose phosphate pathway (oxPPP) (Herrero-Mendez et al., 2009). In the oxPPP, glucose oxidation converts [NADP<sup>+</sup>] to [NADPH], which is of vital importance as a reducing equivalent to replenish the pool of reduced glutathione (GSH) in order to maintain redox homeostasis in neurons (Herrero-Mendez et al., 2009).

Given this reciprocal regulation of glycolysis and the oxPPP, we hypothesized that the reduced glycolytic flux was part of a glucose rerouting towards the oxPPP. Measuring the differential <sup>14</sup>CO<sub>2</sub> production upon incubation with [6-<sup>14</sup>C]-glucose (producing <sup>14</sup>CO<sub>2</sub> only in the TCA cycle) or [1-<sup>14</sup>C]-glucose (producing <sup>14</sup>CO<sub>2</sub> in both the TCA cycle and oxPPP), revealed a 2.8-fold induction in the absolute flux levels of the oxPPP in PHD1<sup>-/-</sup> neurons (Figure 4A). When corrected for the glycolytic flux levels (see methods), the relative increase in oxPPP was 8.7-fold (n = 4). These findings indicated that, in the absence of PHD1, more glucose from glycolysis was redirected towards the oxPPP.

### Molecular regulation of the oxPPP by PHD1 deficiency

The observed decrease in glucose oxidation in PHD1<sup>-/-</sup> neurons might result in an accumulation of glycolytic intermediates, which could increase “passive” shunting to the oxPPP. However, this would be expected to occur only if glucose uptake would be maintained or increased, but glucose consumption was reduced in PHD1<sup>-/-</sup> neurons (Fig. 3B). Also, measurements of the intracellular levels of various glycolytic intermediates such as glucose-6-phosphate, fructose-6-phosphate, fructose-1,6-biphosphate and phosphoenolpyruvate were not increased in PHD1<sup>-/-</sup> neurons (Figure S4A), arguing against passive overflow of glycolytic intermediates into the PPP flux.

We therefore explored additional molecular mechanisms via which PHD1 deficiency increased the oxPPP. An increase in oxPPP could be due to changes in the expression or activity of glucose-6-phosphate dehydrogenase (G6PD), a rate-limiting enzyme of the oxPPP. However, we did not detect genotypic differences in *G6pd* mRNA levels (mRNA copies per 10<sup>3</sup> copies *β-actin*: 0.88 ± 0.07 for WT *versus* 0.81 ± 0.08 for PHD1<sup>-/-</sup>; n = 3; p = NS) or G6PD activity (nmol NADH/min/mg protein: 0.433 ± 0.109 for WT *versus* 0.432 ± 0.109 for PHD1<sup>-/-</sup>; n = 4; p = NS). These findings do not exclude a possibility that G6PD is regulated posttranslationally (Du et al., 2013; Jiang et al., 2011; Rao et al., 2015).

We next studied the expression of enzymes regulating this metabolic crossroad, given the reciprocal effect of PHD1 deficiency on the fluxes through glycolysis and the oxPPP. Phosphofructokinase-2/fructose-2,6-bisphosphatase type III (PFKFB3) allosterically activates phosphofructokinase-1 (PFK-1) by generating fructose-2,6-bisphosphate (F2,6P<sub>2</sub>) and thereby reduces the oxPPP flux (Herrero-Mendez et al., 2009), while TP53-inducible glycolysis and apoptosis regulator (TIGAR), a bisphosphatase enzyme that acts as another putative regulator of the glycolysis/oxPPP crossroad, reduces F2,6P<sub>2</sub> levels and thus redirects glucose carbon away from glycolysis into the oxPPP (Bensaad et al., 2006). Whereas neurons have negligible levels of PFKFB3 (Herrero-Mendez et al., 2009), the function of TIGAR in neurons is poorly characterized. *TIGAR* transcript levels were 2.2-fold higher in PHD1<sup>-/-</sup> than WT neurons (Figure 4B). Notably, silencing of PHD2 or PHD3 did not affect *TIGAR* transcript levels (mRNA copies per 10<sup>3</sup> copies *β-actin*: 0.10 ± 0.01 in ctrl WT, 0.11 ± 0.02 in PHD2<sup>KD</sup> and 0.11 ± 0.01 in PHD3<sup>KD</sup> neurons, p = NS), identifying TIGAR as a specific transcriptional target of PHD1. TIGAR also functionally regulated the oxPPP flux, since overexpression of TIGAR, using a lentiviral vector encoding TIGAR, in WT neurons increased the oxPPP levels (Figure S4B), while silencing of TIGAR in PHD1<sup>-/-</sup> neurons by transduction with a lentiviral vector expressing a TIGAR-specific shRNA (reducing mRNA levels by 74–82%) reduced the oxPPP flux (Figure S4C). Thus, PHD1 deficiency increased the oxPPP flux through regulation of TIGAR expression.

### PHD1 deficiency improves the ROS scavenging capacity in neurons

A prominent function of the oxPPP in non-proliferating cells is to provide the cell with NADPH, which is used as a reducing equivalent by glutathione reductase to regenerate reduced glutathione after oxidation (Stanton, 2012). Reduced glutathione is a major anti-oxidant in neurons (Dringen, 2000), used as cofactor for glutathione peroxidase to detoxify H<sub>2</sub>O<sub>2</sub> to H<sub>2</sub>O. An increased oxPPP flux would thus imply an improved scavenging capacity of H<sub>2</sub>O<sub>2</sub>. Such an enhanced redox potential would be beneficial to protect neurons against the oxidative stress accompanying neuronal ischemia (Chan, 2001; Moskowitz et al., 2010). To explore this possibility, we exposed neurons, labeled with CM-H<sub>2</sub>DCF (an indicator dye of ROS levels), to 100 μM H<sub>2</sub>O<sub>2</sub> and measured ROS levels over time. Compared to WT neurons, PHD1<sup>-/-</sup> neurons showed a less steep increase in CM-H<sub>2</sub>DCF fluorescence intensity over time (Figure 4C), implying accelerated detoxification of the administered H<sub>2</sub>O<sub>2</sub> molecules. Notably, the lower ROS levels upon the H<sub>2</sub>O<sub>2</sub> stress challenge were not accompanied by reduced MitoSox levels (a commonly used read-out of mitochondrial superoxide production (Mukhopadhyay et al., 2007)) in baseline conditions in PHD1<sup>-/-</sup> neurons (Figure S4D–F), arguing against a reduced production of ROS in these cells.

Next, we investigated whether the enhanced oxPPP flux, via accelerating glutathione recycling, was responsible for the improved ROS scavenging capacity. We therefore reduced the oxPPP flux by silencing G6PD (Figure S4G). Lentiviral transduction with a G6PD-specific shRNA, inducing a knockdown efficiency of 80–90% at the mRNA level, reduced the oxPPP flux in PHD1<sup>-/-</sup> neurons (Figure S4H). Notably, G6PD silencing decreased the scavenging capacity to a larger extent in PHD1<sup>-/-</sup> than WT neurons (Figure 4D), suggesting that the improved ROS scavenging capacity of PHD1<sup>-/-</sup> neurons was dependent, at least in part, on an increased oxPPP flux. Gene expression analysis of various anti-oxidant enzymes

did not show enhanced expression of the most prevalent anti-oxidant-enzymes in neurons (Table S3).

### PHD1 deficiency maintains a residual oxPPP flux in hypoxia

For the oxPPP to provide the necessary redox equivalents for neuroprotection during oxygen deprivation (as occurs during stroke), it should remain operational during hypoxia in PHD1<sup>-/-</sup> neurons. Given the reciprocal regulation of glycolysis and oxPPP, we explored how hypoxia would affect the flux through glycolysis and the oxPPP. In various non-neuronal cell types, hypoxia induces a HIF-1 $\alpha$ -mediated increase in glycolytic flux (Aragones et al., 2009). Likewise, we observed an elevated glycolytic flux upon hypoxic exposure of cultured neurons (Figure 4E). Even though PHD1<sup>-/-</sup> neurons responded to hypoxia by increasing glycolytic flux, the glycolytic flux rate remained lower in hypoxic PHD1<sup>-/-</sup> than WT neurons (Figure 4E). When analyzing the oxPPP, we observed that hypoxia almost nullified the oxPPP flux in WT neurons, while PHD1<sup>-/-</sup> neurons were still able to maintain a residual oxPPP flux, nearly in the range of normoxic WT neurons (Figure 4F). These data suggest that PHD1 deficiency in neurons attenuated the typical hypoxia-induced metabolic shift, in which glycolysis is normally increased and the oxPPP flux is reduced. By reprogramming glucose metabolism and maintaining a residual flux through the oxPPP, PHD1 deficiency thus ensured a low but vital residual level of redox homeostasis, especially during ischemic challenges. Of note, in hypoxia, glucose and glutamine oxidation were reduced in WT and PHD1<sup>-/-</sup> neurons when compared to normoxic conditions, but the genotypic differences were maintained (Figure S4I–J). Also mitochondrial oxygen consumption was not affected by PHD1 deficiency upon combined nutrient deprivation and hypoxia-mimetic DMOG treatment (Figure S4K).

To demonstrate that the increased oxPPP flux and improved capacity to scavenge oxygen radicals in PHD1<sup>-/-</sup> neurons is relevant for redox homeostasis also during reperfusion, we measured oxidized glutathione (GSSG) versus reduced glutathione (GSH) after 2 hours of oxygen-nutrient deprivation. This analysis revealed that, while GSSG levels (% of GSSG + GSH) in WT neurons gradually increased over time, the redox state in PHD1<sup>-/-</sup> neurons was maintained as GSSG levels increased only slightly (Figure 4G).

### Confirmation of the PHD1-deficient phenotype in other models

For the characterization of the metabolic phenotype described so far, we used embryonic cortical neurons, cultured for 7 days *in vitro* (DIV), a well established and widely used neuronal culture model (Lesuisse and Martin, 2002; Meberg and Miller, 2003). As an additional approach to address the relevance of the metabolic phenotype, we also used “aged” embryonic cortical neurons, cultured for 21 DIV, when they had differentiated into fully mature cortical neurons, as a surrogate model of adult neurons (Lesuisse and Martin, 2002; Martin et al., 2008). Similar to 7 DIV cortical neurons, PHD1 deficiency in aged neuronal cultures reduced the glycolytic flux (by  $25 \pm 0.5$  %;  $n = 4$ ;  $p < 0.05$ ) and increased oxPPP flux (by  $2.2 \pm 0.4$  fold;  $n = 3$ ;  $p < 0.05$ ).

We next sought to confirm the metabolic phenotype of the increased oxPPP flux in PHD1<sup>-/-</sup> neurons in the brain *in vivo*. The study of neuronal metabolism *in vivo* is challenging given

the presence of and intricate (metabolic) interactions with other cell types (astrocytes, oligodendrocytes, endothelial cells) that in most regions of the brain greatly outnumber the neurons. Measuring metabolic fluxes in the entire brain therefore suffers from the inevitable limitation that it will not reflect neuronal metabolism solely. In order to minimize the contribution of non-neuronal metabolism, we studied metabolism in the hippocampus, which is, similar to the cortex, a telencephalic brain region, with however a higher neuron/glia ratio than in most other brain regions (Geisert et al., 2002; Herculano-Houzel et al., 2006; Herculano-Houzel et al., 2013). Using previously established methods (Ayala et al., 2006; Buescher et al., 2015), we intravenously infused [1,2-<sup>13</sup>C]-glucose during 6 hours in adult conscious and unrestrained mice and microdissected the hippocampi. Next, we measured the mass isotopomer distribution in pentose-5-phosphate sugars (pool of ribose-5-P and other pentoses) at the interface between the oxPPP and non-oxPPP. We used the ratio of the M+1 versus M+2 labeling of pentose-5-phosphate as an indicative parameter of the relative importance of the oxPPP versus the non-oxPPP (Figure 5A). In PHD1<sup>-/-</sup> hippocampi, the M +1 versus M+2 labeling of pentose-5-phosphates was enriched more than in WT hippocampi (0.97 ± 0.03 in PHD1<sup>-/-</sup> versus 0.87 ± 0.01 in WT; n = 4–5; p < 0.05). Thus, similar to the metabolic phenotype in cultured neurons, the relative importance of the oxPPP was increased in the neuron-enriched hippocampus of PHD1<sup>-/-</sup> mice *in vivo*.

We also assayed if PHD1 deficiency improved the anti-oxidant capacity *in vivo*. We therefore measured GSSG levels (% of total glutathione) in dissected brain hemispheres after ischemic stroke. This analysis revealed that, compared to their WT counterparts, PHD1<sup>-/-</sup> mice showed lower oxidized glutathione levels in the ischemic hemisphere, indicating that PHD1 deficiency enables the ischemic brain to maintain better its redox homeostasis (Figure 5B). Notably, the magnitude of the observed genotypic difference is likely an underestimation given the contamination of healthy (non-stroked) brain tissue in the measured ischemic hemisphere.

### Ischemic protection in PHD1<sup>-/-</sup> neurons is HIF-independent

We then explored the molecular mechanism downstream of PHD1 deficiency. PHDs are best known for their hydroxylating activity of proline residues in target proteins. However, hydroxylation-independent activities are being increasingly recognized (Wong et al., 2013). Therefore, we first investigated whether the phenotypic effects of PHD1 deficiency relied on PHD1's hydroxylase activity. To this end, we transduced PHD1<sup>-/-</sup> neurons with a lentiviral vector expressing either wild type PHD1 (PHD1<sup>WT</sup>) or a hydroxylase-inactive PHD1 mutant (PHD1<sup>D311A</sup> (McNeill et al., 2002)). RT-PCR revealed that expression of the transduced PHD1 (WT and D311A mutant) resulted in PHD1 levels in the range of endogenous PHD1 levels in WT neurons (Figure S5A). Re-expression of PHD1<sup>WT</sup>, but not PHD1<sup>D311A</sup>, in PHD1<sup>-/-</sup> neurons aggravated neuronal death compared to control PHD1<sup>-/-</sup> neurons in the oxygen-nutrient deprivation assay (Figure 6A), indicating that inhibition of the hydroxylation activity of PHD1 is necessary and sufficient for its neuroprotective effect.

Next, we explored the involvement of HIF-1α or HIF-2α, the two best-characterized hydroxylation targets of PHDs. In different biological processes, HIF-1α and/or HIF-2α mediate the effects of PHD deficiency, even though HIF-independent effects have been

increasingly recognized (Kaelin and Ratcliffe, 2008; Wong et al., 2013). Given the lack of PHD1 activity in normoxic PHD1<sup>-/-</sup> neurons, one would expect increased levels of HIF-1 $\alpha$  and HIF-2 $\alpha$ . Immunoblotting showed however that protein levels of HIF-1 $\alpha$  were not elevated in normoxic PHD1<sup>-/-</sup> neurons or PHD1<sup>-/-</sup> brain (Figure 6B,C). Furthermore, we did not detect differences in the expression levels of the HIF-1 $\alpha$  transcriptional targets *Vegfa*, *Enolase* and *Pdk1* (Figure S5B). These findings are in agreement with previous reports that loss of PHD1 did not result in HIF-1 $\alpha$  accumulation in the brain (Chen et al., 2012), liver (Schneider et al., 2009), muscle (Aragones et al., 2008) or cancer cells (Zhang et al., 2009). HIF-2 $\alpha$  protein was not detectable. PHD1 deficiency did not interfere with the hypoxic stabilization of HIF-1 $\alpha$ , as evidenced by a similar increase in HIF-1 $\alpha$  protein levels and HIF-1 $\alpha$  transcriptional targets in hypoxia (Figure 6B; Figure S5B). Notably, silencing of neither HIF-1 $\alpha$  nor HIF-2 $\alpha$  affected *TIGAR* transcript levels in PHD1<sup>-/-</sup> neurons (mRNA copies per 10<sup>3</sup> copies *HPRT*: 12.2  $\pm$  3.0 in ctrl PHD1<sup>-/-</sup>, 13.1  $\pm$  2.8 in HIF-1 $\alpha$ <sup>KD</sup> PHD1<sup>-/-</sup> and 12.7  $\pm$  3.4 in HIF-2 $\alpha$ <sup>KD</sup> PHD1<sup>-/-</sup> neurons, n = 5, p = NS).

Additionally, we assessed the effect of silencing HIF-1 $\alpha$ , HIF-2 $\alpha$  or HIF-1 $\beta$  (which prevents dimerization with HIF- $\alpha$  and thereby blocks the activity of both HIF-1 $\alpha$  and HIF-2 $\alpha$ ) on the protection of PHD1<sup>-/-</sup> neurons, by using lentiviral vectors expressing a shRNA specific for each of these genes (resulting in a decrease of *HIF-1 $\alpha$* , *HIF-2 $\alpha$*  or *HIF-1 $\beta$*  mRNA levels by 65–82%). Silencing of HIF-1 $\alpha$  or HIF-2 $\alpha$  did not abolish the protection against oxygen-nutrient deprivation by PHD1 deficiency (Figure 6D). HIF-independency was further demonstrated by the finding that silencing of HIF-1 $\beta$  did also not affect the neuroprotective effect induced by PHD1 loss (Figure 6E). Taken together, these data suggest a HIF-independent mechanism of the PHD1-mediated protection.

### Possible molecular mechanism of PHD1 deficiency

We then sought to provide further initial insight into the underlying molecular mechanism. Reduced PHD1 activity has been linked to enhanced NF- $\kappa$ B activity in several non-neuronal cell lines and types, putatively via reduced hydroxylation and hence reduced degradation of I- $\kappa$ B kinase 2 (IKK2) (Adluri et al., 2011; Cummins et al., 2006; Cummins et al., 2008; Winning et al., 2010; Xue et al., 2010). IKK2 activates the NF- $\kappa$ B pathway by phosphorylation of I $\kappa$ B $\alpha$ , chaperone of the NF- $\kappa$ B transcription factor p65, resulting in degradation of I $\kappa$ B $\alpha$  and hence release of p65. However, whether NF- $\kappa$ B signaling is affected by PHD1 and regulates metabolism in neurons remains unaddressed. We therefore transduced WT and PHD1<sup>-/-</sup> neurons with a lentiviral vector, expressing a NF- $\kappa$ B luciferase reporter. This analysis showed that PHD1 deficiency increased the NF- $\kappa$ B promoter activity (Figure 6F), and protein levels of p65 (Figure 6G). Furthermore, silencing of *RelA* (p65) reduced the oxPPP flux and *TIGAR* levels in PHD1<sup>-/-</sup> neurons (Figure 6H,I).

### ICV delivery of anti-PHD1 oligonucleotides protects against brain ischemia

Finally, we explored the translational potential of PHD1 inhibition in ischemic stroke. PHD1 inhibition might be an attractive target for different reasons. First, genetic deletion of PHD1 yielded pronounced protection against brain ischemia. Second, PHD1 loss does not result in major physiological deficits in mice, as shown in previous studies (Aragones et al., 2008; Schneider et al., 2009). This may suggest that PHD1-specific inhibitors might have a more

favorable safety profile than available aspecific PHD inhibitors. To test the effect of PHD1 specific inhibition in the brain, we used anti-sense oligonucleotides (ASOs) with 2'-*O*-methoxyethyl (2'MOE) chemistry. A library of ASOs was screened for targeting murine PHD1 and, out of three different ASOs, we selected the ASO with the highest knockdown efficiency and specificity for our *in vivo* studies. Incubation of cultured cortical neurons with the selected anti-PHD1 ASO for 5 days resulted in a PHD1 knockdown efficiency of 84%, without affecting transcript or protein levels of PHD2 or PHD3 (Figure 7A,B).

In a next step, we investigated the feasibility of *in vivo* delivery of these ASOs. Since the blood-brain barrier is not permeable for ASOs (Broaddus et al., 2000; Cossum et al., 1993; Kordasiewicz et al., 2012; Smith et al., 2006), we delivered them ICV via osmotic pumps as previously described (Storkebaum et al., 2005). The oligonucleotides were continuously infused over the course of 2 weeks at a rate of 75 µg/day (this dose was selected in pilot experiments). The animals tolerated this treatment well and no premature deaths or other signs of toxicity were noted. After 2 weeks, brains were harvested and PHD1 mRNA levels were assessed. This analysis showed that ICV delivery of anti-PHD1 ASOs lowered PHD1 mRNA levels in the brain (Figure 7C).

Using this regimen, we tested the effect of ASO delivery on the response to brain ischemia. Mice treated for 2 weeks with anti-PHD1 ASOs underwent a permanent ligation of their middle cerebral artery and infarct size was assessed 24 hours later. Mice with ICV delivery of saline or a control ASO were used as control groups. The control ASO was directed against human huntingtin mRNA and was chemically modified to prevent any RNase H-mediated effects. Infarct size analysis showed a 50% reduction in stroke lesion upon treatment with the anti-PHD1 ASO (Figure 7D–G). There was no difference in stroke size between saline and control ASO groups, demonstrating that injection of an ASO per se did not cause additional effects that would influence stroke outcome. Similar to the results in mice with a genetic PHD1 deletion, mice treated with anti-PHD1 oligonucleotides showed an improved performance in the adhesive tape removal test. Following pMCAO, the delay in time to sense and remove the tape on the affected side was less pronounced in the mice treated with anti-PHD1 ASO (Figure 7H,I), indicative of an improved sensorimotor coordination.

## Discussion

The novel findings of our study are that the oxygen sensor PHD1 is an important regulator of neuronal metabolism, providing protection against ischemic redox imbalance.

### PHD1 orchestrates neuronal glucose metabolism

Neurons rely on oxidative glucose metabolism in healthy conditions (Harris et al., 2012; Mergenthaler et al., 2013), but the metabolic adaptations during stroke have remained largely enigmatic. We demonstrate that PHD1 is a key orchestrator of adaptive glucose metabolism in neurons, and is instrumental in preparing neurons for a protective response against an ischemic insult. Unexpectedly, at least based on previous results that PHD1 deficiency induces a shift towards glycolysis in other cell types (Aragones et al., 2009; Quaegebeur and Carmeliet, 2010), this ischemia tolerance in PHD1<sup>-/-</sup> neurons relies on an

increase in the oxPPP at the expense of glycolysis. This reprogramming of glucose metabolism in baseline conditions prepares neurons better against ischemia by providing a greater capacity for scavenging oxygen radicals.

This mechanism is strikingly different from (even opposite to) the mechanism whereby PHD1 controls ischemia tolerance in muscle fibers and hepatocytes (Aragones et al., 2008; Schneider et al., 2009). Indeed, in these cells, PHD1 deficiency induces a switch from oxidative to anaerobic metabolism as a means of oxygen-independent energy generation and reduction of mitochondrial ROS production, thereby protecting these organs against ischemia (Aragones et al., 2008; Schneider et al., 2009). By contrast, oxygen consumption was not affected in PHD1<sup>-/-</sup> neurons and, instead of an increase in glycolysis, they rather showed a reduction in glycolytic flux. Interestingly, the ischemia tolerance in PHD1<sup>-/-</sup> myocytes and hepatocytes relied on HIF-activation (Aragones et al., 2009; Schneider et al., 2009), while this was not the case in PHD1<sup>-/-</sup> neurons. Hence, PHD1 has a distinct role in neurons as compared to other cell types, and neurons reprogram their metabolism in a (perhaps even unique) PHD1-dependent manner, which has only been identified in neurons to date.

Neurons lacking PHD1 shunted more glucose into the oxPPP. This pathway represents an alternative route for glucose besides glycolysis, and is critical for redox homeostasis by generating NADPH, necessary to replenish reduced glutathione (Stanton, 2012). In agreement, PHD1<sup>-/-</sup> neurons had an improved capacity to scavenge oxygen radicals, which was negatively affected upon oxPPP blockade by G6PD silencing. Given the widely held notion that oxidative stress in brain ischemia is heavily intertwined in the pathological cascade of events leading to neuronal death (Chan, 2001; Moskowitz et al., 2010), the increase in oxPPP flux can confer protection in this context. Importantly, PHD1 deficiency did not only promote the oxPPP flux in normoxic but also in hypoxic conditions, and better preserved the redox state of glutathione during reperfusion. In fact, unlike WT neurons, PHD1<sup>-/-</sup> neurons still had a residual flux through the oxPPP during hypoxia. Even though smaller than in normoxia, this residual flux was of vital importance to secure sufficient redox homeostasis during hypoxic stress. These findings identify PHD1 as a regulator of the oxPPP and the associated oxygen radical scavenging capacity.

The role of the PPP in stroke has received little attention. G6PD is the rate-limiting enzyme of the oxPPP, which is upregulated in ischemia (Li et al., 2014), while TIGAR promotes the oxPPP at the expense of glycolysis. In line with our findings, inhibition of the oxPPP flux by silencing G6PD aggravated stroke outcome (Zhao et al., 2012), while TIGAR protects ischemic brain injury, though oxPPP flux measurements were not performed in this study (Cao et al., 2015; Li et al., 2014). Some evidence suggests a contextual role of the PPP, attributing opposing fates to NADPH. As a reducing co-factor of glutathione reductase, NADPH improves the anti-oxidant capacity, but as an electron donor of NADPH oxidase, NADPH can also generate superoxides (Bedard and Krause, 2007; Stanton, 2012), explaining the divergent effects of PPP manipulation on ischemic neuroprotection (Brennan et al., 2009; Herrero-Mendez et al., 2009; Suh et al., 2008; Zhao et al., 2012). Regardless of these additional possible effects, regulation of the oxPPP by PHD1 resulted in improved – not impaired – anti-oxidant capacity.

## The neuroprotective effect of PHD1 loss is not due to vascular changes

Stroke outcome is determined by the extent of the collateral circulation (Shuaib et al., 2011). Upon acute occlusion of the middle cerebral artery, pial collateral vessels can, via retrograde filling, still supply brain regions distal to the occlusion, alleviating the drop in perfusion (Brozici et al., 2003). We did not find any effect of PHD1 deficiency on the number of pial collaterals or arterioles. Also, the fraction of perfused vessels was not affected in the PHD1<sup>-/-</sup> brain, in baseline conditions or after stroke. Importantly, MRI-imaging after stroke revealed a similar perfusion deficit in WT and PHD1<sup>-/-</sup> brains, while the T2 lesion size was smaller in PHD1<sup>-/-</sup> brains. The lack of a clear vascular phenotype in PHD1<sup>-/-</sup> brains is compatible with findings in other PHD1<sup>-/-</sup> organs, in which vascular effects were not observed either (Aragones et al., 2008; Schneider et al., 2009). In agreement, a single study assessing vessel density in the PHD1<sup>-/-</sup> brain, also did not report any difference (Chen et al., 2012).

## Mechanisms of oxPPP regulation by PHD1

In a search for molecular mechanisms to explain the increased oxPPP in PHD1<sup>-/-</sup> neurons, we identified NF-κB signaling downstream of PHD1. While this has been observed in other non-neuronal cell types (Adluri et al., 2011; Cummins et al., 2006; Cummins et al., 2008; Winning et al., 2010; Xue et al., 2010), our study implies a new role of NF-κB signaling downstream of PHD1 in the regulation of the oxPPP flux in neurons. In line with our findings, NF-κB signaling has been reported to lower glycolysis (Mauro et al., 2011).

Our findings also indicate that the neuroprotective effect of PHD1 deficiency relies on the hydroxylation activity of PHD1, but not on HIF-signaling, likely because HIF-1α levels are more importantly controlled by PHD2 than by PHD1 (Appelhoff et al., 2004; Myllyharju, 2013). Another reason why HIF-1α levels were not upregulated in PHD1<sup>-/-</sup> neurons may relate to the finding that ROS levels were decreased in PHD1<sup>-/-</sup> neurons. Since ROS are known to inactivate PHDs (Quaegebeur and Carmeliet, 2010), reduced ROS levels are expected to enhance the activity of residual PHD2 and PHD3, which would favor the degradation of HIF-1α. Hence, this mechanism is expected to counteract any possible upregulation of HIF-1α by loss of PHD1. The maintained HIF-1α levels in PHD1<sup>-/-</sup> neurons may also contribute to explain why glycolysis was not increased in these cells. Hence, the reduced ROS levels in PHD1<sup>-/-</sup> neurons are not only beneficial for an improved redox homeostasis, but also further reinforce in a feedback the rerouting of glucose from a reduced glycolysis to an increased oxPPP.

## Ischemia tolerance in PHD1<sup>-/-</sup> brain: distinct from hibernation?

We also considered if basal hypometabolism might explain the ischemia tolerance in PHD1<sup>-/-</sup> neurons, separate from active re-routing of glucose towards the oxPPP, as several lines of evidence in the literature suggest such a link. First, various hibernating animal species developed mechanisms to cope with oxygen starvation, i.e. by depressing oxidative metabolism (often by lowering oxygen consumption by more than 50-fold) and by reducing protein synthesis and other energy-consuming processes (Fraisl et al., 2009; Larson et al., 2014). Second, in the mammalian brain, hypometabolism has been implicated in ischemic preconditioning by eliciting a hibernation-like phenomenon (Bernaudin et al., 2002; Dirnagl

et al., 2003; Stenzel-Poore et al., 2003), even though a direct contribution to neuroprotection in acute ischemic events remains outstanding. Third, hypoxia signaling has been involved in some metabolic adaptations, leading to energy hypometabolism (Bernaudin et al., 2002; Fraisl et al., 2009; Gidday, 2006; Quaegebeur and Carmeliet, 2010). And fourth, inhibition of PHD1 in muscle evokes a shift from oxidative to anaerobic (glycolytic) metabolism in order to ensure hypoxia tolerance (Aragones et al., 2008).

However, despite all this reported evidence, the ischemia tolerance of PHD1<sup>-/-</sup> neurons is different from, even in contrast to, the aforementioned phenomena. Indeed, loss of PHD1 in neurons is *not* accompanied by a reduction in oxygen consumption or energy conservation (as evidenced by the maintained Na<sup>+</sup>/K<sup>+</sup> pump activity, dendritic branching, protein and RNA synthesis). Although we formally cannot exclude a slight energy hypometabolism in PHD1<sup>-/-</sup> neurons (below the detection threshold of our techniques), we were not able to pick up substantial genotypic differences in several assays when measuring energy consumption and production by direct and more indirect (functional) read-outs. Instead, PHD1 deficiency in neurons is characterized by reduced glycolysis, but increased oxPPP and glutamine oxidation, and maintained lactate oxidation and oxygen consumption, i.e. metabolic changes that are largely opposite to those accompanying hypometabolism during hibernation or ischemic preconditioning. Hence, the metabolic adaptation of PHD1<sup>-/-</sup> neurons, in preparation of coping with a future drop in oxygen and nutrient supply, relies on a distinct reprogramming of cellular metabolism, not previously recognized in other cell types to date.

### Possible implications for other neurological disorders

Interestingly, in cell culture and animal models of neurodegenerative disorders, signs of increased glycolysis have been sporadically described (D'Alessandro et al., 2011; Ferreira et al., 2011; Rodriguez-Rodriguez et al., 2012; Yao et al., 2009). This raises the question whether a similar detrimental metabolic shift is taking place in these conditions, *i.e.*, increasing glycolysis and thereby depleting neurons of their vitally important PPP flux. However, this exciting possibility remains speculative at this stage, as PPP flux alterations in neurodegenerative disorders have yet to be investigated.

Finally, do these findings have any translational relevance? Non-specific PHD inhibitors are neuroprotective in acute neurotoxic settings such as stroke (Karuppagounder and Ratan, 2012; Nagel et al., 2010; Quaegebeur and Carmeliet, 2010). However, their lack of specificity and the increased risk of eliciting adverse effects when blocking various dioxygenases render clinical translation more challenging. Instead, our findings show that loss of PHD1 alone sufficed to reduce infarct size by 70% and nearly completely prevented the functional sensorimotor deficits after stroke, an observation that persisted over a protracted period of time.

Interestingly, preventive silencing of PHD1 by intracerebroventricular delivery of antisense oligonucleotides prior to stroke induction was protective against brain ischemia, thus phenocopying the genetic data. However, a clinically more relevant strategy would be to administer a PHD1 inhibitor after stroke onset. Unfortunately, we had no access to a PHD1-selective chemical inhibitor to test how rapidly PHD1 blockade would induce ischemia

tolerance via metabolic reprogramming. Despite this limitation, our prevention studies raise the intriguing but outstanding question if PHD1 inhibition might be clinically useful to diminish neuronal damage in conditions, where the risk of cerebral ischemia is considered high, such as upon a critical carotid stenosis or following a subarachnoid hemorrhage, though possible clinical benefit of such strategy awaits further study.

A therapeutic strategy based on blocking PHD1 may also differ from existing stroke treatments relying on blocking oxygen radicals by administration of anti-oxidants. Indeed, many of those treatments neglected the importance of physiological signaling functions of oxygen radicals in neurons, likely explaining in part years of translational failure (Moskowitz et al., 2010). PHD1 inhibition is in this regard a fundamentally different and perhaps more appealing approach, since it relies on switching on an endogenous protective mechanism with potentially pleiotropic actions. Future research will have to clarify whether PHD1 inhibition would also be a valid neuroprotective target when initiated after stroke onset. The development and characterization of selective (preferably blood brain barrier-permeable) PHD1 inhibitors will be crucial in shaping clinical indications for PHD1 inhibition and directing further studies.

## Experimental procedures

More detailed methods are described in the Supplement.

### Mouse strains

PHD1<sup>-/-</sup> (Aragones et al., 2008), PHD2<sup>lox/lox</sup> (Mazzone et al., 2009) and PHD3<sup>-/-</sup> (Aragones et al., 2008) mice were previously described. PHD2<sup>lox/lox</sup> mice were intercrossed with Nestin-Cre mice (Tronche et al., 1999) to obtain neural specific PHD2 deficient mice. Housing and experimental animal procedures were approved by the Institutional Animal Care and Research Advisory Committee of the University of Leuven, Belgium.

### Ischemic stroke model

Brain ischemia was induced using the permanent middle cerebral artery occlusion (pMCAO) model as further detailed in Supplement (Kuraoka et al., 2009). Infarct size was analyzed at 24 hours after ischemia by vital dye staining of 1-mm coronal brain slices (Bederson et al., 1986), and infarction area was calculated as the ratio of the unstained area over the total bihemispheric area, using Image J. Functional impact of the stroke was tested using the adhesive tape removal test (Bouet et al., 2009).

### Brain vasculature analysis

Large arteries and arterioles were analyzed using immunohistology for  $\alpha$ SMA; vessel perfusion after tail vein injection with fluorescein isothiocyanate (FITC)-conjugated dextran; pial collateral circulation via vascular corrosion casting (Krucker et al., 2006) and counting of the number of collaterals per hemisphere. The stroke-induced perfusion deficit in the brain was measured by magnetic resonance imaging at 2 and 24 hours after pMCAO.

### **Murine cortical neurons culture and treatment**

Cortical neurons were prepared from the cortices of embryonic day 14.5 or 15.5 mice, pooled from one litter (Thathiah et al., 2009). Gene silencing was done after 2 days in culture using gene-specific lentiviral shRNA vectors (Sigma). Oxygen-nutrient deprivation was initiated after 7 days in culture by exposure for 2 hours to 0.1% oxygen in nutrient-deprived medium followed by re-exposure to ambient air and regular medium as further detailed in the Supplement.

### **Metabolic flux assays, redox and energy homeostasis**

Glycolysis, glucose oxidation, oxidative pentose phosphate pathway (oxPPP), glutamine oxidation, and lactate oxidation were measured using radiolabeled tracer glucose, glutamine or lactate as further detailed in the Supplement. Glucose consumption was defined as the difference in glucose concentration in medium after 48 hours and was measured via liquid chromatography-mass spectrometry (LC-MS). Oxygen consumption rate (OCR) was measured using the extracellular flux analyzer XF24 (Seahorse Bioscience Inc.). ROS scavenging in H<sub>2</sub>O<sub>2</sub>-treated cells was measured using 5-(and-6)-chloromethyl-2',7'-dichlorodihydrofluorescein diacetate (CM-H<sub>2</sub>-DCFDA, Molecular Probes, Invitrogen). GSSG/GSH levels were determined using LC-MS. ATP/ADP/AMP levels were determined using HPLC. Intracellular Na<sup>+</sup> concentration was monitored using SBFI-based microfluorimetry.

### **Immunocytochemistry**

was done on cortical neurons grown for 7 days on Willco-Dish glass bottom dishes (Ibidi), using the antibodies listed in the Supplement.

### **RNA, DNA and protein analysis**

Gene expression analysis was performed by Taqman quantitative RT-PCR, using premade primer sets (Applied Biosystems). The amount of mitochondrial DNA relative to nuclear genomic DNA was determined by quantitative PCR using primers for cytochrome b (mitochondrial) and RPL13A (nuclear). Immunoblotting was done using the antibodies listed in the Supplement with signal detection using the ECL system (Amersham Biosciences, GE Healthcare).

### **ICV delivery of antisense oligonucleotides against PHD1 in stroke**

Antisense oligonucleotides (ASOs) directed against the murine PHD1 mRNA were designed and purified by Isis Pharmaceuticals. Mice were treated with ASOs by intraventricular infusion for 10 days using Alzet® osmotic pumps (Cupertino) connected with a catheter to a brain infusion cannula, as detailed in the Supplement. Two weeks after the infusion, pMCAO was performed.

### **Statistics**

All data are mean ± SEM of the indicated number of experiments or mice, unless otherwise noted (median). For the *in vitro* data, the “n” values indicate the number of independent experiments performed with different cultures of WT and PHD1<sup>-/-</sup> cortical neurons

(independent isolations). For the *in vivo* experiments, two-sided Student's t-tests were used and done using Prism v5.0, considering  $p < 0.05$  statistically significant. In some PHD1<sup>-/-</sup> mice, no infarct was visible after ligation of the middle cerebral artery (indicating complete protection against brain ischemia), thereby disturbing normal Gaussian distribution. In these cases, we used non-parametrical Mann-Whitney-U test to determine statistical differences between the two groups. For *in vivo* experiments, investigators were blinded for treatment or genotype. For *in vitro* experiments, statistical significance between groups was calculated on n pooled independent experiments using linear mixed-effect model statistics to correct for effects by inter-experimental variation (Schoors et al., 2015). Calculations were done using R (Team, 2008) and the lme4 package (Bates et al., 2014). In all cases, the condition was entered as fixed effect. P-values were obtained with the Kenward-Roger F-test for small mixed effect model datasets (Kenward and Roger, 1997) using lmerTest package (Kuznetsova et al., 2014). Again,  $p < 0.05$  was considered statistically significant. For the time course experiments with CM-H<sub>2</sub>DCF fluorescence, we used linear mixed-effect model statistics to determine the slope and statistical differences between slopes.

## Supplementary Material

Refer to Web version on PubMed Central for supplementary material.

## Acknowledgments

We acknowledge the assistance of the technical staff and the VRC core facilities (VIB/KU Leuven, Belgium). AQ, IS, BG, KDB and SMF are supported by The Research Foundation–Flanders (FWO). ID and FB are supported by a FP7 Marie Curie Intra-European Fellowship (IEF). RS is supported by Pegasus Marie Curie-FWO. RL is a Senior Clinical Investigator of FWO Flanders. BC and SS are funded by the Agency for Innovation by Science and Technology in Flanders (IWT). The work of PC is supported by a Federal Government Belgium grant (IUAP P7/03), long-term structural Methusalem funding by the Flemish Government, grants from the FWO (G.0671.12N, 1.5.244.11N) and the Foundation Leducq Transatlantic Network (ARTEMIS), funding by “A cure for ALS” from ALS Liga Belgium, Motor Neuron Disease Association, ALS Association (ID#C44128), Euro-MOTOR (EU HEALTH project) and by the Leuven University Fund - Opening the Future.

## References

- Adluri RS, Thirunavukkarasu M, Dunna NR, Zhan L, Oriowo B, Takeda K, Sanchez JA, Otani H, Maulik G, Fong GH, et al. Disruption of hypoxia-inducible transcription factor-prolyl hydroxylase domain-1 (PHD-1<sup>-/-</sup>) attenuates ex vivo myocardial ischemia/reperfusion injury through hypoxia-inducible factor-1alpha transcription factor and its target genes in mice. 2011; 15:1789–1797.
- Appelhoff RJ, Tian YM, Raval RR, Turley H, Harris AL, Pugh CW, Ratcliffe PJ, Gleadle JM. Differential function of the prolyl hydroxylases PHD1, PHD2, and PHD3 in the regulation of hypoxia-inducible factor. J Biol Chem. 2004; 279:38458–38465. [PubMed: 15247232]
- Aragones J, Fraisl P, Baes M, Carmeliet P. Oxygen sensors at the crossroad of metabolism. Cell Metab. 2009; 9:11–22. [PubMed: 19117543]
- Aragones J, Schneider M, Van Geyte K, Fraisl P, Dresselaers T, Mazzone M, Dirckx R, Zacchigna S, Lemieux H, Jeoung NH, et al. Deficiency or inhibition of oxygen sensor Phd1 induces hypoxia tolerance by reprogramming basal metabolism. 2008; 40:170–180. [PubMed: 18176562]
- Ayala JE, Bracy DP, McGuinness OP, Wasserman DH. Considerations in the design of hyperinsulinemic-euglycemic clamps in the conscious mouse. Diabetes. 2006; 55:390–397. [PubMed: 16443772]
- Barone FC, Knudsen DJ, Nelson AH, Feuerstein GZ, Willette RN. Mouse strain differences in susceptibility to cerebral ischemia are related to cerebral vascular anatomy. J Cereb Blood Flow Metab. 1993; 13:683–692. [PubMed: 8314921]

- Bates D, Maechler M, Bolker B, Walker S. lme4: Linear mixed-effects models using Eigen and S4. 2014
- Bedard K, Krause KH. The NOX family of ROS-generating NADPH oxidases: physiology and pathophysiology. *Physiol Rev.* 2007; 87:245–313. [PubMed: 17237347]
- Bederson JB, Pitts LH, Germano SM, Nishimura MC, Davis RL, Bartkowski HM. Evaluation of 2,3,5-triphenyltetrazolium chloride as a stain for detection and quantification of experimental cerebral infarction in rats. *Stroke.* 1986; 17:1304–1308. [PubMed: 2433817]
- Belanger M, Allaman I, Magistretti PJ. Brain energy metabolism: focus on astrocyte-neuron metabolic cooperation. *Cell Metab.* 2011; 14:724–738. [PubMed: 22152301]
- Bensaad K, Tsuruta A, Selak MA, Vidal MN, Nakano K, Bartrons R, Gottlieb E, Vousden KH. TIGAR, a p53-inducible regulator of glycolysis and apoptosis. *Cell.* 2006; 126:107–120. [PubMed: 16839880]
- Bernaudin M, Tang Y, Reilly M, Petit E, Sharp FR. Brain genomic response following hypoxia and re-oxygenation in the neonatal rat. Identification of genes that might contribute to hypoxia-induced ischemic tolerance. *J Biol Chem.* 2002; 277:39728–39738. [PubMed: 12145288]
- Bouet V, Boulouard M, Toutain J, Divoux D, Bernaudin M, Schumann-Bard P, Freret T. The adhesive removal test: a sensitive method to assess sensorimotor deficits in mice. *Nat Protoc.* 2009; 4:1560–1564. [PubMed: 19798088]
- Brennan AM, Suh SW, Won SJ, Narasimhan P, Kauppinen TM, Lee H, Edling Y, Chan PH, Swanson RA. NADPH oxidase is the primary source of superoxide induced by NMDA receptor activation. *Nat Neurosci.* 2009; 12:857–863. [PubMed: 19503084]
- Broadus WC, Prabhu SS, Wu-Pong S, Gillies GT, Fillmore H. Strategies for the design and delivery of antisense oligonucleotides in central nervous system. *Methods Enzymol.* 2000; 314:121–135. [PubMed: 10565009]
- Brozici M, van der Zwan A, Hillen B. Anatomy and functionality of leptomeningeal anastomoses: a review. *Stroke.* 2003; 34:2750–2762. [PubMed: 14576375]
- Buescher JM, Antoniewicz MR, Boros LG, Burgess SC, Brunengraber H, Clish CB, DeBerardinis RJ, Feron O, Frezza C, Ghesquiere B, et al. A roadmap for interpreting (13)C metabolite labeling patterns from cells. *Curr Opin Biotechnol.* 2015; 34:189–201. [PubMed: 25731751]
- Cao L, Chen J, Li M, Qin YY, Sun M, Sheng R, Han F, Wang G, Qin ZH. Endogenous level of TIGAR in brain is associated with vulnerability of neurons to ischemic injury. *Neurosci Bull.* 2015
- Chan PH. Reactive oxygen radicals in signaling and damage in the ischemic brain. *J Cereb Blood Flow Metab.* 2001; 21:2–14. [PubMed: 11149664]
- Chen RL, Nagel S, Papadakis M, Bishop T, Pollard P, Ratcliffe PJ, Pugh CW, Buchan AM. Roles of individual prolyl-4-hydroxylase isoforms in the first 24 hours following transient focal cerebral ischaemia: insights from genetically modified mice. *J Physiol.* 2012; 590:4079–4091. [PubMed: 22615432]
- Connolly ES Jr, Winfree CJ, Stern DM, Solomon RA, Pinsky DJ. Procedural and strain-related variables significantly affect outcome in a murine model of focal cerebral ischemia. *Neurosurgery.* 1996; 38:523–531. discussion 532. [PubMed: 8837805]
- Cossum PA, Sasmor H, Dellinger D, Truong L, Cummins L, Owens SR, Markham PM, Shea JP, Crooke S. Disposition of the 14C-labeled phosphorothioate oligonucleotide ISIS 2105 after intravenous administration to rats. *J Pharmacol Exp Ther.* 1993; 267:1181–1190. [PubMed: 8166890]
- Cui L, Jeong H, Borovecki F, Parkhurst CN, Tanese N, Krainc D. Transcriptional repression of PGC-1alpha by mutant huntingtin leads to mitochondrial dysfunction and neurodegeneration. *Cell.* 2006; 127:59–69. [PubMed: 17018277]
- Cummins EP, Berra E, Comerford KM, Ginouves A, Fitzgerald KT, Seeballuck F, Godson C, Nielsen JE, Moynagh P, Pouyssegur J, et al. Prolyl hydroxylase-1 negatively regulates IκappaB kinase-beta, giving insight into hypoxia-induced NFκappaB activity. *Proc Natl Acad Sci U S A.* 2006; 103:18154–18159. [PubMed: 17114296]
- Cummins EP, Seeballuck F, Keely SJ, Mangan NE, Callanan JJ, Fallon PG, Taylor CT. The hydroxylase inhibitor dimethylxalylglycine is protective in a murine model of colitis. 2008; 134:156–165.

- D'Alessandro G, Calcagno E, Tartari S, Rizzardini M, Invernizzi RW, Cantoni L. Glutamate and glutathione interplay in a motor neuronal model of amyotrophic lateral sclerosis reveals altered energy metabolism. *Neurobiol Dis.* 2011; 43:346–355. [PubMed: 21530659]
- DeBerardinis RJ, Cheng T. Q's next: the diverse functions of glutamine in metabolism, cell biology and cancer. *Oncogene.* 2010; 29:313–324. [PubMed: 19881548]
- Dirnagl U, Simon RP, Hallenbeck JM. Ischemic tolerance and endogenous neuroprotection. *Trends Neurosci.* 2003; 26:248–254. [PubMed: 12744841]
- Dringen R. Metabolism and functions of glutathione in brain. *Prog Neurobiol.* 2000; 62:649–671. [PubMed: 10880854]
- Du W, Jiang P, Mancuso A, Stonestrom A, Brewer MD, Minn AJ, Mak TW, Wu M, Yang X. TAp73 enhances the pentose phosphate pathway and supports cell proliferation. *Nat Cell Biol.* 2013; 15:991–1000. [PubMed: 23811687]
- Fang EF, Scheibye-Knudsen M, Brace LE, Kassahun H, SenGupta T, Nilsen H, Mitchell JR, Croteau DL, Bohr VA. Defective mitophagy in XPA via PARP-1 hyperactivation and NAD(+)/SIRT1 reduction. *Cell.* 2014; 157:882–896. [PubMed: 24813611]
- Ferez KB, Gast RE, Rose K, Finger IE, Hasche A, Kriegstein J. Nerve growth factor and brain-derived neurotrophic factor but not granulocyte colony-stimulating factor, nimodipine and dizocilpine, require ATP for neuroprotective activity after oxygen-glucose deprivation of primary neurons. *Brain Res.* 2012; 1448:20–26. [PubMed: 22386494]
- Ferreira IL, Cunha-Oliveira T, Nascimento MV, Ribeiro M, Proenca MT, Janeiro C, Oliveira CR, Rego AC. Bioenergetic dysfunction in Huntington's disease human cybrids. *Exp Neurol.* 2011; 231:127–134. [PubMed: 21684277]
- Fraisl P, Aragonés J, Carmeliet P. Inhibition of oxygen sensors as a therapeutic strategy for ischaemic and inflammatory disease. 2009
- Fujii M, Hara H, Meng W, Vonsattel JP, Huang Z, Moskowitz MA. Strain-related differences in susceptibility to transient forebrain ischemia in SV-129 and C57black/6 mice. *Stroke.* 1997; 28:1805–1810. discussion 1811. [PubMed: 9303029]
- Geisert EE Jr, Williams RW, Geisert GR, Fan L, Asbury AM, Maecker HT, Deng J, Levy S. Increased brain size and glial cell number in CD81-null mice. *J Comp Neurol.* 2002; 453:22–32. [PubMed: 12357429]
- Ghesquiere B, Wong BW, Kuchnio A, Carmeliet P. Metabolism of stromal and immune cells in health and disease. *Nature.* 2014; 511:167–176. [PubMed: 25008522]
- Gidday JM. Cerebral preconditioning and ischaemic tolerance. *Nat Rev Neurosci.* 2006; 7:437–448. [PubMed: 16715053]
- Harris JJ, Jolivet R, Attwell D. Synaptic energy use and supply. *Neuron.* 2012; 75:762–777. [PubMed: 22958818]
- Herculano-Houzel S, Mota B, Lent R. Cellular scaling rules for rodent brains. *Proc Natl Acad Sci U S A.* 2006; 103:12138–12143. [PubMed: 16880386]
- Herculano-Houzel S, Watson C, Paxinos G. Distribution of neurons in functional areas of the mouse cerebral cortex reveals quantitatively different cortical zones. *Front Neuroanat.* 2013; 7:35. [PubMed: 24155697]
- Herrero-Mendez A, Almeida A, Fernandez E, Maestre C, Moncada S, Bolanos JP. The bioenergetic and antioxidant status of neurons is controlled by continuous degradation of a key glycolytic enzyme by APC/C-Cdh1. 2009; 11:747–752.
- Howarth C, Gleeson P, Attwell D. Updated energy budgets for neural computation in the neocortex and cerebellum. *J Cereb Blood Flow Metab.* 2012; 32:1222–1232. [PubMed: 22434069]
- Jiang P, Du W, Wang X, Mancuso A, Gao X, Wu M, Yang X. p53 regulates biosynthesis through direct inactivation of glucose-6-phosphate dehydrogenase. *Nat Cell Biol.* 2011; 13:310–316. [PubMed: 21336310]
- Jolivet R, Allaman I, Pellerin L, Magistretti PJ, Weber B. Comment on recent modeling studies of astrocyte-neuron metabolic interactions. *J Cereb Blood Flow Metab.* 2010; 30:1982–1986. [PubMed: 20700131]
- Kaelin WG Jr, Ratcliffe PJ. Oxygen sensing by metazoans: the central role of the HIF hydroxylase pathway. *Mol Cell.* 2008; 30:393–402. [PubMed: 18498744]

- Karuppagounder SS, Ratan RR. Hypoxia-inducible factor prolyl hydroxylase inhibition: robust new target or another big bust for stroke therapeutics? *J Cereb Blood Flow Metab.* 2012; 32:1347–1361. [PubMed: 22415525]
- Kenward MG, Roger JH. Small sample inference for fixed effects from restricted maximum likelihood. *Biometrics.* 1997; 53:983–997. [PubMed: 9333350]
- Klumpp S, Kriha D, Bechmann G, Maassen A, Maier S, Pallast S, Hoell P, Kriegelstein J. Phosphorylation of the growth factors bFGF, NGF and BDNF: a prerequisite for their biological activity. *Neurochem Int.* 2006; 48:131–137. [PubMed: 16242215]
- Knight AL, Yan X, Hamamichi S, Ajjuri RR, Mazzulli JR, Zhang MW, Daigle JG, Zhang S, Borom AR, Roberts LR, et al. The glycolytic enzyme, GPI, is a functionally conserved modifier of dopaminergic neurodegeneration in Parkinson's models. *Cell Metab.* 2014; 20:145–157. [PubMed: 24882066]
- Koh JY, Choi DW. Quantitative determination of glutamate mediated cortical neuronal injury in cell culture by lactate dehydrogenase efflux assay. *J Neurosci Methods.* 1987; 20:83–90. [PubMed: 2884353]
- Kordasiewicz HB, Stanek LM, Wancewicz EV, Mazur C, McAlonis MM, Pytel KA, Artates JW, Weiss A, Cheng SH, Shihabuddin LS, et al. Sustained therapeutic reversal of Huntington's disease by transient repression of huntingtin synthesis. *Neuron.* 2012; 74:1031–1044. [PubMed: 22726834]
- Krucker T, Lang A, Meyer EP. New polyurethane-based material for vascular corrosion casting with improved physical and imaging characteristics. *Microsc Res Tech.* 2006; 69:138–147. [PubMed: 16456839]
- Kuraoka M, Furuta T, Matsuwaki T, Omatsu T, Ishii Y, Kyuwa S, Yoshikawa Y. Direct experimental occlusion of the distal middle cerebral artery induces high reproducibility of brain ischemia in mice. *Exp Anim.* 2009; 58:19–29. [PubMed: 19151508]
- Kuznetsova A, Bruun Brockhoff P, Christensen RHB. lmerTest: Tests for random and fixed effects for linear mixed effect models (lmer objects of lme4 package). 2014
- Larson J, Drew KL, Folkow LP, Milton SL, Park TJ. No oxygen? No problem! Intrinsic brain tolerance to hypoxia in vertebrates. *J Exp Biol.* 2014; 217:1024–1039. [PubMed: 24671961]
- Lesuisse C, Martin LJ. Long-term culture of mouse cortical neurons as a model for neuronal development, aging, and death. *J Neurobiol.* 2002; 51:9–23. [PubMed: 11920724]
- Li M, Sun M, Cao L, Gu JH, Ge J, Chen J, Han R, Qin YY, Zhou ZP, Ding Y, et al. A TIGAR-regulated metabolic pathway is critical for protection of brain ischemia. *J Neurosci.* 2014; 34:7458–7471. [PubMed: 24872551]
- Lo EH, Dalkara T, Moskowitz MA. Mechanisms, challenges and opportunities in stroke. *Nat Rev Neurosci.* 2003; 4:399–415. [PubMed: 12728267]
- Majid A, He YY, Gidday JM, Kaplan SS, Gonzales ER, Park TS, Fenstermacher JD, Wei L, Choi DW, Hsu CY. Differences in vulnerability to permanent focal cerebral ischemia among 3 common mouse strains. *Stroke.* 2000; 31:2707–2714. [PubMed: 11062298]
- Mangia S, DiNuzzo M, Giove F, Carruthers A, Simpson IA, Vannucci SJ. Response to 'comment on recent modeling studies of astrocyte-neuron metabolic interactions': much ado about nothing. *J Cereb Blood Flow Metab.* 2011; 31:1346–1353. [PubMed: 21427731]
- Martin MG, Perga S, Trovo L, Rasola A, Holm P, Rantamaki T, Harkany T, Castren E, Chiara F, Dotti CG. Cholesterol loss enhances TrkB signaling in hippocampal neurons aging in vitro. *Mol Biol Cell.* 2008; 19:2101–2112. [PubMed: 18287532]
- Mauro C, Leow SC, Anso E, Rocha S, Thotakura AK, Tornatore L, Moretti M, De Smaele E, Beg AA, Tergaonkar V, et al. NF-kappaB controls energy homeostasis and metabolic adaptation by upregulating mitochondrial respiration. *Nat Cell Biol.* 2011; 13:1272–1279. [PubMed: 21968997]
- Mazzone M, Dettori D, Leite de Oliveira R, Loges S, Schmidt T, Jonckx B, Tian YM, Lanahan AA, Pollard P, Ruiz de Almodovar C, et al. Heterozygous deficiency of PHD2 restores tumor oxygenation and inhibits metastasis via endothelial normalization. *Cell.* 2009; 136:839–851. [PubMed: 19217150]
- McNeill LA, Hewitson KS, Gleadle JM, Horsfall LE, Oldham NJ, Maxwell PH, Pugh CW, Ratcliffe PJ, Schofield CJ. The use of dioxygen by HIF prolyl hydroxylase (PHD1). 2002; 12:1547–1550.

- Meberg PJ, Miller MW. Culturing hippocampal and cortical neurons. *Methods Cell Biol.* 2003; 71:111–127. [PubMed: 12884689]
- Meloni BP, Meade AJ, Kitikomolsuk D, Knuckey NW. Characterisation of neuronal cell death in acute and delayed in vitro ischemia (oxygen-glucose deprivation) models. *J Neurosci Methods.* 2011; 195:67–74. [PubMed: 21134398]
- Mergenthaler P, Lindauer U, Dienel GA, Meisel A. Sugar for the brain: the role of glucose in physiological and pathological brain function. *Trends Neurosci.* 2013; 36:587–597. [PubMed: 23968694]
- Morais VA, Haddad D, Craessaerts K, De Bock PJ, Swerts J, Vilain S, Aerts L, Overbergh L, Grunewald A, Seibler P, et al. PINK1 loss-of-function mutations affect mitochondrial complex I activity via Ndufa10 ubiquinone uncoupling. *Science.* 2014; 344:203–207. [PubMed: 24652937]
- Moskowitz MA, Lo EH, Iadecola C. The science of stroke: mechanisms in search of treatments. 2010; 67:181–198.
- Mukhopadhyay P, Rajesh M, Hasko G, Hawkins BJ, Madesh M, Pacher P. Simultaneous detection of apoptosis and mitochondrial superoxide production in live cells by flow cytometry and confocal microscopy. *Nat Protoc.* 2007; 2:2295–2301. [PubMed: 17853886]
- Myllyharju J. Prolyl 4-hydroxylases, master regulators of the hypoxia response. *Acta Physiol (Oxf).* 2013; 208:148–165. [PubMed: 23489300]
- Nagel S, Talbot NP, Mecinovic J, Smith TG, Buchan AM, Schofield CJ. Therapeutic manipulation of the HIF hydroxylases. *Antioxid Redox Signal.* 2010; 12:481–501. [PubMed: 19754349]
- Oruganty-Das A, Ng T, Udagawa T, Goh EL, Richter JD. Translational control of mitochondrial energy production mediates neuron morphogenesis. *Cell Metab.* 2012; 16:789–800. [PubMed: 23217258]
- Quaegebeur A, Carmeliet P. Oxygen sensing: a common crossroad in cancer and neurodegeneration. *Curr Top Microbiol Immunol.* 2010; 345:71–103. [PubMed: 20582529]
- Rao X, Duan X, Mao W, Li X, Li Z, Li Q, Zheng Z, Xu H, Chen M, Wang PG, et al. O-GlcNAcylation of G6PD promotes the pentose phosphate pathway and tumor growth. *Nat Commun.* 2015; 6:8468. [PubMed: 26399441]
- Rodriguez-Rodriguez P, Almeida A, Bolanos JP. Brain energy metabolism in glutamate-receptor activation and excitotoxicity: role for APC/C-Cdh1 in the balance glycolysis/pentose phosphate pathway. *Neurochem Int.* 2013; 62:750–756. [PubMed: 23416042]
- Rodriguez-Rodriguez P, Fernandez E, Almeida A, Bolanos JP. Excitotoxic stimulus stabilizes PFKFB3 causing pentose-phosphate pathway to glycolysis switch and neurodegeneration. *Cell Death Differ.* 2012; 19:1582–1589. [PubMed: 22421967]
- Sakanaka M, Wen TC, Matsuda S, Masuda S, Morishita E, Nagao M, Sasaki R. In vivo evidence that erythropoietin protects neurons from ischemic damage. *Proc Natl Acad Sci U S A.* 1998; 95:4635–4640. [PubMed: 9539790]
- Schneider M, van Geyte K, Fraisl P, Kiss J, Aragonés J, Mazzone M, Mairbaurl H, Debock K, Ho Jeung N, Mollenhauer M, et al. Loss or silencing of the PHD1 prolyl hydroxylase protects livers of mice against ischemia/reperfusion injury. 2009
- Schoors S, Bruning U, Missiaen R, Queiroz KC, Borgers G, Elia I, Zecchin A, Cantelmo AR, Christen S, Goveia J, et al. Fatty acid carbon is essential for dNTP synthesis in endothelial cells. *Nature.* 2015; 520:192–197. [PubMed: 25830893]
- Schulze A, Harris AL. How cancer metabolism is tuned for proliferation and vulnerable to disruption. *Nature.* 2012; 491:364–373. [PubMed: 23151579]
- Semenza GL. Oxygen sensing, homeostasis, and disease. *N Engl J Med.* 2011; 365:537–547. [PubMed: 21830968]
- Shuaib A, Butcher K, Mohammad AA, Saqqur M, Liebeskind DS. Collateral blood vessels in acute ischaemic stroke: a potential therapeutic target. *Lancet Neurol.* 2011; 10:909–921. [PubMed: 21939900]
- Siren AL, Fratelli M, Brines M, Goemans C, Casagrande S, Lewczuk P, Keenan S, Gleiter C, Pasquali C, Capobianco A, et al. Erythropoietin prevents neuronal apoptosis after cerebral ischemia and metabolic stress. *Proc Natl Acad Sci U S A.* 2001; 98:4044–4049. [PubMed: 11259643]

- Smith RA, Miller TM, Yamanaka K, Monia BP, Condon TP, Hung G, Lobsiger CS, Ward CM, McAlonis-Downes M, Wei H, et al. Antisense oligonucleotide therapy for neurodegenerative disease. *J Clin Invest.* 2006; 116:2290–2296. [PubMed: 16878173]
- Stanton RC. Glucose-6-phosphate dehydrogenase, NADPH, and cell survival. *IUBMB Life.* 2012; 64:362–369. [PubMed: 22431005]
- Stenzel-Poore MP, Stevens SL, Xiong Z, Lessov NS, Harrington CA, Mori M, Meller R, Rosenzweig HL, Tobar E, Shaw TE, et al. Effect of ischaemic preconditioning on genomic response to cerebral ischaemia: similarity to neuroprotective strategies in hibernation and hypoxia-tolerant states. 2003; 362:1028–1037.
- Storkebaum E, Lambrechts D, Dewerchin M, Moreno-Murciano MP, Appelmans S, Oh H, Van Damme P, Rutten B, Man WY, De Mol M, et al. Treatment of motoneuron degeneration by intracerebroventricular delivery of VEGF in a rat model of ALS. *Nat Neurosci.* 2005; 8:85–92. [PubMed: 15568021]
- Suh SW, Shin BS, Ma H, Van Hoecke M, Brennan AM, Yenari MA, Swanson RA. Glucose and NADPH oxidase drive neuronal superoxide formation in stroke. *Ann Neurol.* 2008; 64:654–663. [PubMed: 19107988]
- Takeda K, Ho VC, Takeda H, Duan LJ, Nagy A, Fong GH. Placental but not heart defects are associated with elevated hypoxia-inducible factor alpha levels in mice lacking prolyl hydroxylase domain protein 2. 2006; 26:8336–8346. [PubMed: 16966370]
- Team, RDC. R: A Language and Environment for Statistical Computing. Vienna, Austria: R Foundation for Statistical Computing; 2008.
- Thathiah A, Spittaels K, Hoffmann M, Staes M, Cohen A, Horre K, Vanbrabant M, Coun F, Baekelandt V, Delacourte A, et al. The orphan G protein-coupled receptor 3 modulates amyloid-beta peptide generation in neurons. *Science.* 2009; 323:946–951. [PubMed: 19213921]
- Tronche F, Kellendonk C, Kretz O, Gass P, Anlag K, Orban PC, Bock R, Klein R, Schutz G. Disruption of the glucocorticoid receptor gene in the nervous system results in reduced anxiety. *Nat Genet.* 1999; 23:99–103. [PubMed: 10471508]
- Tufi R, Gandhi S, de Castro IP, Lehmann S, Angelova PR, Dinsdale D, Deas E, Plun-Favreau H, Nicotera P, Abramov AY, et al. Enhancing nucleotide metabolism protects against mitochondrial dysfunction and neurodegeneration in a PINK1 model of Parkinson's disease. *Nat Cell Biol.* 2014; 16:157–166. [PubMed: 24441527]
- Vander Heiden MG, Cantley LC, Thompson CB. Understanding the Warburg effect: the metabolic requirements of cell proliferation. *Science.* 2009; 324:1029–1033. [PubMed: 19460998]
- Winning S, Spletstoesser F, Fandrey J, Frede S. Acute hypoxia induces HIF-independent monocyte adhesion to endothelial cells through increased intercellular adhesion molecule-1 expression: the role of hypoxic inhibition of prolyl hydroxylase activity for the induction of NF-kappa B. 2010; 185:1786–1793.
- Wong BW, Kuchnio A, Bruning U, Carmeliet P. Emerging novel functions of the oxygen-sensing prolyl hydroxylase domain enzymes. *Trends Biochem Sci.* 2013; 38:3–11. [PubMed: 23200187]
- Xue J, Li X, Jiao S, Wei Y, Wu G, Fang J. Prolyl hydroxylase-3 is down-regulated in colorectal cancer cells and inhibits IKKbeta independent of hydroxylase activity. *Gastroenterology.* 2010; 138:606–615. [PubMed: 19786027]
- Yao J, Irwin RW, Zhao L, Nilsen J, Hamilton RT, Brinton RD. Mitochondrial bioenergetic deficit precedes Alzheimer's pathology in female mouse model of Alzheimer's disease. *Proc Natl Acad Sci U S A.* 2009; 106:14670–14675. [PubMed: 19667196]
- Zhang H, Prabhakar P, Sealock R, Faber JE. Wide genetic variation in the native pial collateral circulation is a major determinant of variation in severity of stroke. *J Cereb Blood Flow Metab.* 2010; 30:923–934. [PubMed: 20125182]
- Zhang Q, Gu J, Li L, Liu J, Luo B, Cheung HW, Boehm JS, Ni M, Geisen C, Root DE, et al. Control of cyclin D1 and breast tumorigenesis by the EglN2 prolyl hydroxylase. 2009; 16:413–424.
- Zhao G, Zhao Y, Wang X, Xu Y. Knockdown of glucose-6-phosphate dehydrogenase (G6PD) following cerebral ischemic reperfusion: the pros and cons. *Neurochem Int.* 2012; 61:146–155. [PubMed: 22580330]

### Highlights

1. Genetic loss of PHD1 provides a substantial protection against brain ischemic injury
2. This did not rely on vascular changes, but on reprogramming of glucose metabolism
3. Increased oxPPP flux, at the expense of glycolysis, offered enhanced redox balance
4. Intracerebroventricular delivery of anti-PHD1 oligos offered protection in stroke

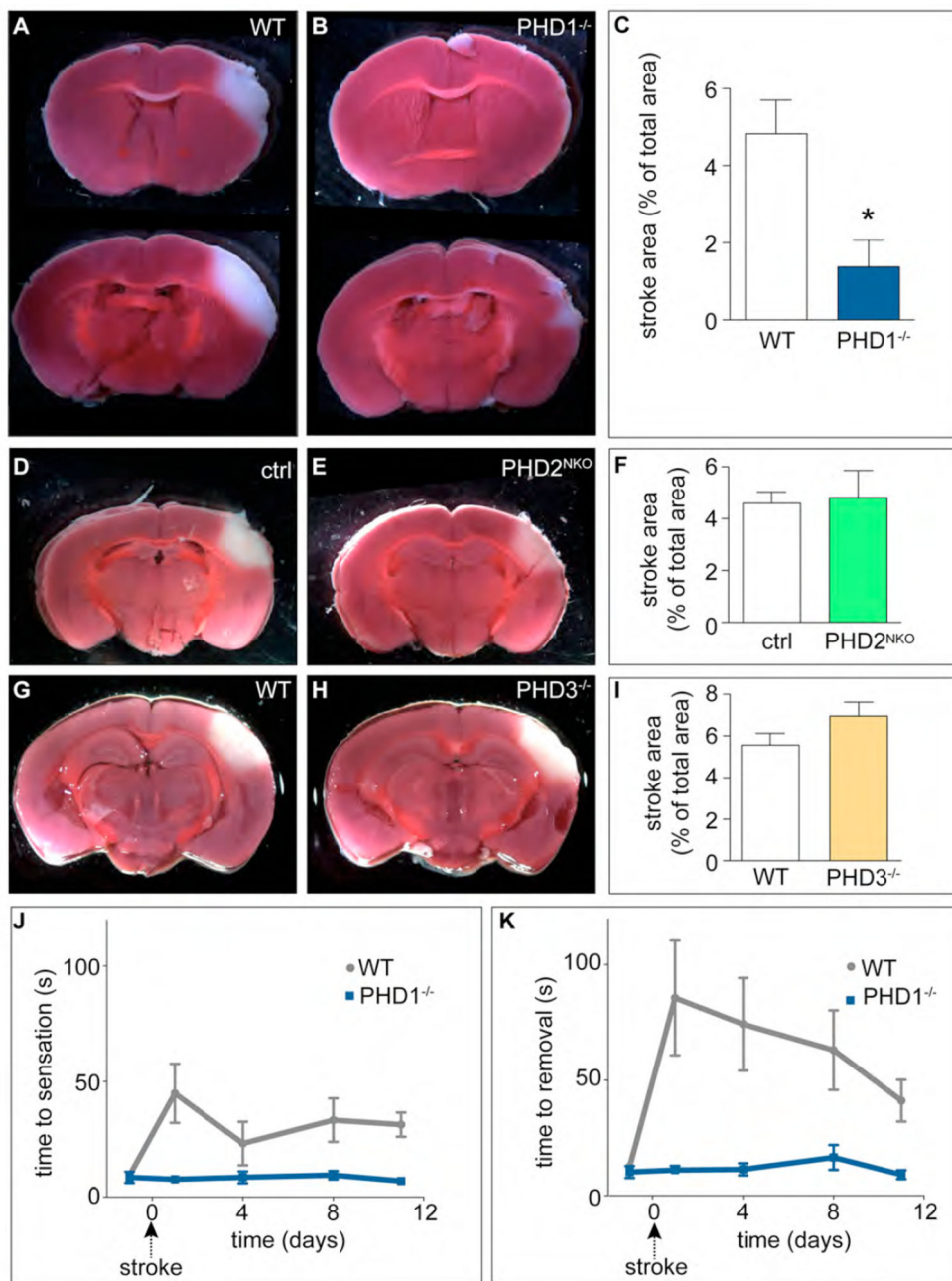


### Figure 1. PHD1 deficiency protects against permanent brain ischemia

**A,B,** Representative consecutive brain slices after TTC staining, delineating the infarct zone as unstained area (white), from wild type (WT) (A) and PHD1<sup>-/-</sup> mice (B) 24 hours after pMCAO. **C,** Quantification of the stroke area as percentage of the total bihemispheric area for PHD1<sup>-/-</sup> versus WT mice (n = 6, \* p < 0.05 by Mann-Whitney U test; difference in medians: -5.29 versus WT, 95% CI: -6.14 to -0.96). **D-I,** Representative images of TTC stained brain slices from Nestin-Cre<sup>-</sup> PHD2<sup>lox/lox</sup> (ctrl) (D) versus Nestin-Cre<sup>+</sup> PHD2<sup>lox/lox</sup> mice (PHD2<sup>NKO</sup>) (E) and from WT (G) versus PHD3<sup>-/-</sup> mice (H). Quantification of the

stroke area as percentage of the total bihemispheric area for ctrl *versus* PHD2<sup>NKO</sup> mice (n = 3, p = NS; difference in means: +0.21 *versus* ctrl, 95% CI: -2.95 to 3.38) (F) and for WT *versus* PHD3<sup>-/-</sup> mice (n = 7 for WT mice, n = 8 for PHD3<sup>-/-</sup> mice, p = NS; difference in means: +1.41 *versus* WT, 95% CI: -0.51 to 3.32) (I). **J,K**, Measurements of the adhesive tape removal test at 1 day before and at day 1, 4, 8 and 11 post-stroke. Average time needed before WT (gray, n = 8) and PHD1<sup>-/-</sup> (blue, n = 7) mice sensed the presence of the tape (J) (p < 0.05, repeated-measure ANOVA). Average time needed before the mice successfully removed the tape (K) (n = 8 for WT, n = 7 for PHD1<sup>-/-</sup>, p < 0.05, repeated-measure ANOVA). All quantitative data are mean ± SEM. See also Figure S1.

Author Manuscript

Author Manuscript

Author Manuscript

Author Manuscript

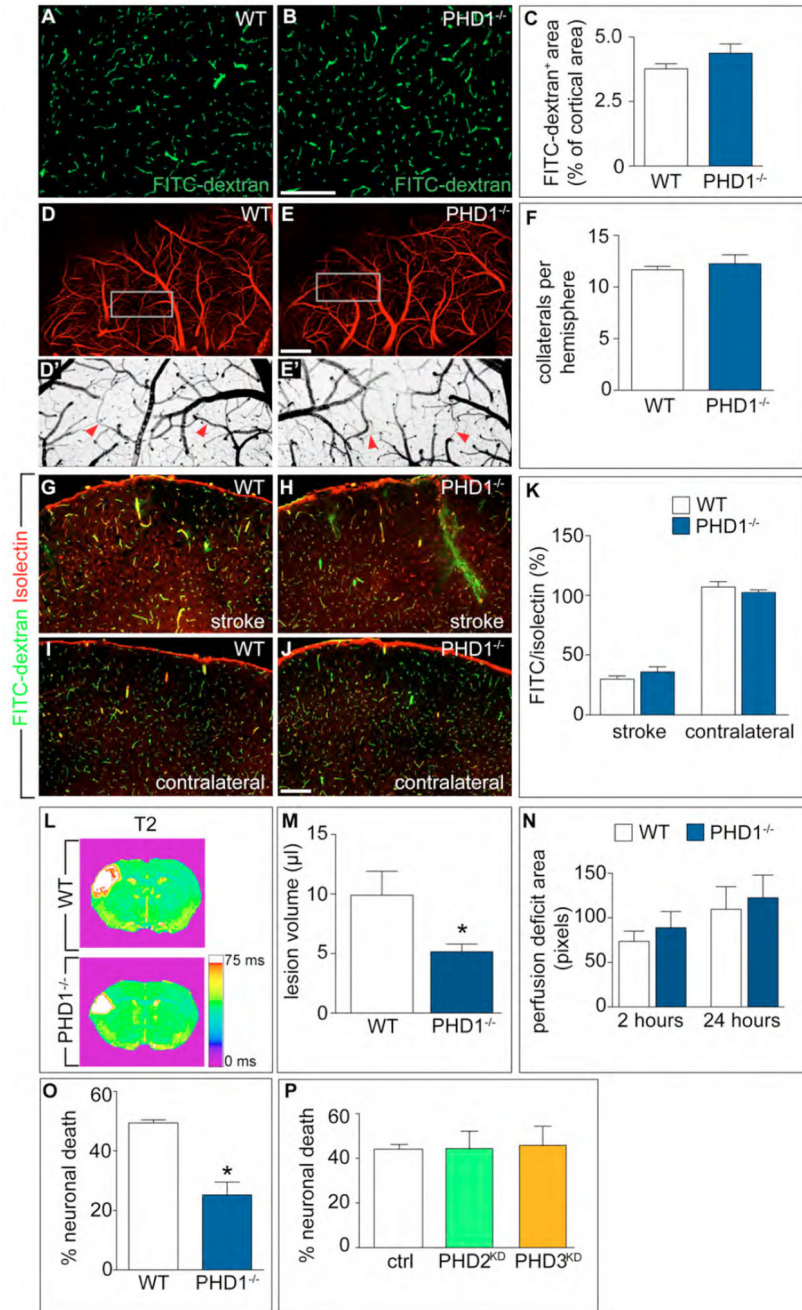


**Figure 2. PHD1 deficiency does not alter the brain vasculature**

**A,B**, Representative images of WT (A) and PHD1<sup>-/-</sup> (B) frontal cortex after FITC-dextran injection. **C**, Quantification of FITC-dextran-positive area as percentage of cortical area (reflecting vessel perfusion in the cortex) (n = 6 for WT, n = 7 for PHD1<sup>-/-</sup>, p = NS; difference in means: +0.60 versus WT, 95% CI: -0.33 to 1.54). **D-E'**, Representative images of three-dimensional corrosion casting showing perfused pial vessels in WT (D) and PHD1<sup>-/-</sup> brain hemisphere (E). D' and E' show larger magnification of the boxed areas in D and E. Collaterals were counted per hemisphere (arrowheads). **F**, Quantification of pial

collaterals per hemisphere in WT *versus* PHD1<sup>-/-</sup> brains (n = 3 for WT, n= 4 for PHD1<sup>-/-</sup> ; p = NS; difference in means: +0.58 *versus* WT, 95% CI: -2.11 to 3.28). **G-J**, Representative images of FITC-dextran (green) and isolectin (red) staining of the stroke area (G,H) and corresponding contralateral cortex area (I,J) of WT (G,I) and PHD1<sup>-/-</sup> brain (H,J). **K**, Quantification of FITC<sup>+</sup> (perfused) vessels, as a percentage of the total number of isolectin<sup>+</sup> vessels in the stroke area and corresponding contralateral cortex area in WT *versus* PHD1<sup>-/-</sup> brains (n = 3 for WT mice, n = 5 for PHD1<sup>-/-</sup> mice, p = NS, difference in means: 6.13 *versus* WT, 95% CI: -8.52 to 20.79 for stroke side, p = NS, difference in means: -4.6 *versus* WT, 95% CI: -15.3 to 6.1 for contralateral side.). **L**, Representative brain T2 parametric maps from *in vivo* MRI of WT and PHD1<sup>-/-</sup> mice 24 hours after pMCAO. **M**, Stroke lesion size (μl), as derived from manual delineation on multi-slice T2-weighted MRI images (n = 4-5, \* p < 0.05; difference in means: -4.74 *versus* WT, 95% CI: -9.24 to -0.24). **N**, Area of the ipsilateral hemisphere with perfusion deficit (defined as CBF that is lower than 80% of the CBF in the contralateral hemisphere) at 2 hours and 24 hours after pMCAO (n = 4 for WT mice, n = 5 for PHD1<sup>-/-</sup> mice, p = NS; difference in means: +15.28 *versus* WT, 95% CI: -9.58 to 40.13 after 2 hours; and difference in means: +12.88 *versus* WT, 95% CI: -27.40 to 53.15 after 24 hours). **O**, Neuronal cell death measured as LDH release (% of maximal LDH release; see methods) over 24 hours after oxygen-nutrient deprivation in WT and PHD1<sup>-/-</sup> neurons *in vitro* (n = 3, \* p < 0.05). **P**, Neuronal cell death, measured by LDH release (% of maximal LDH release) over 24 hours after oxygen-nutrient deprivation in PHD2 silenced (PHD2<sup>KD</sup>) and PHD3 silenced (PHD3<sup>KD</sup>) cells compared to control (n = 3, p = NS). All quantitative data are mean ± SEM. Bars: 200 μm (A,B,G-J), 1 mm (D,E). See also Figure S2 and Table S1.

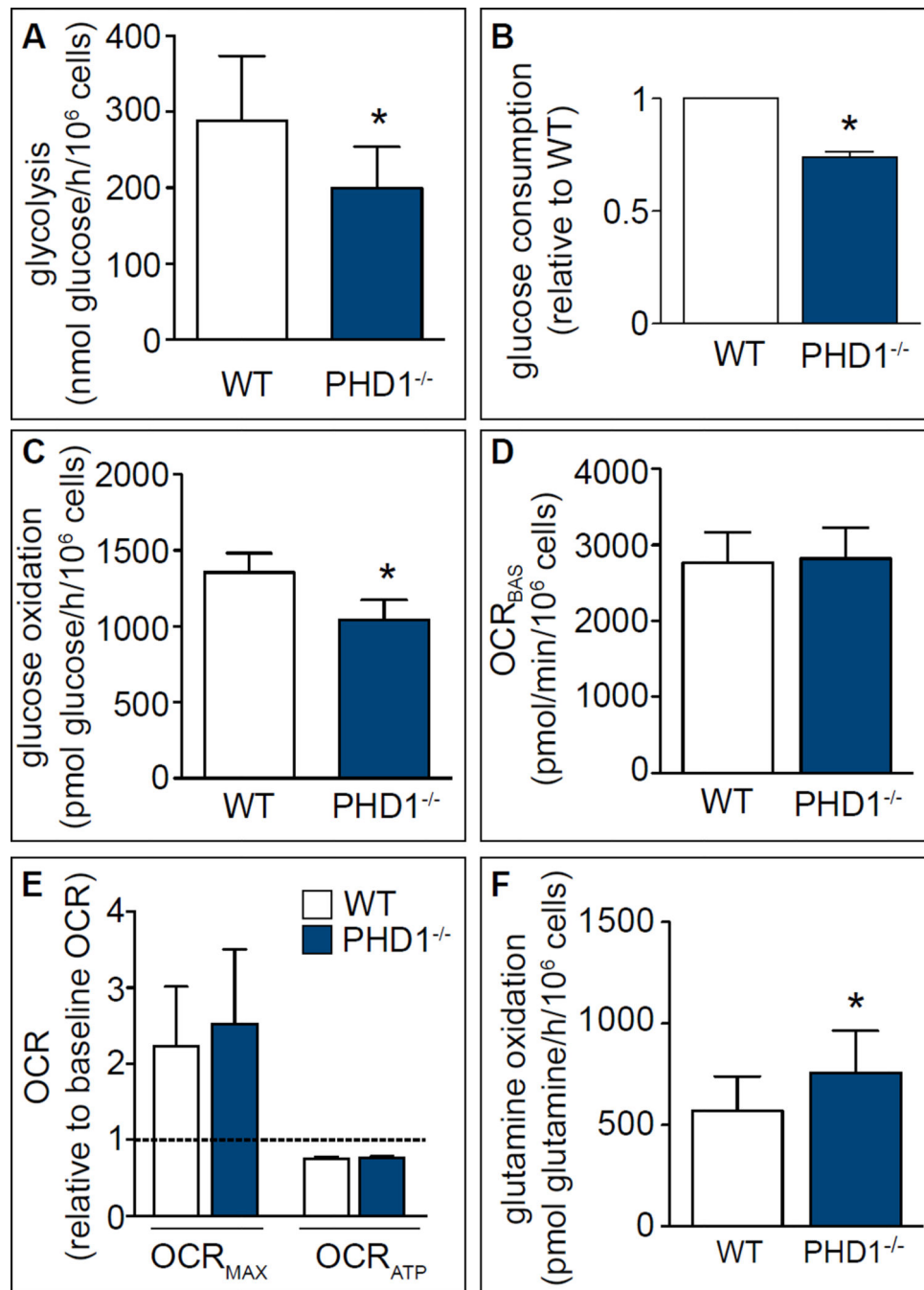


**Figure 3. PHD1 deficiency alters neuronal metabolism**

**A**, Glycolytic flux measured over 2 hours in WT and PHD1<sup>-/-</sup> neurons (n = 8, \* p < 0.05). **B**, Glucose consumption measured over 24 hours in WT and PHD1<sup>-/-</sup> neurons (n = 3, \* p < 0.05). **C**, Glucose oxidation measured over 2 hours in WT and PHD1<sup>-/-</sup> neurons (n = 7, \* p < 0.05). **D**, Mitochondrial OCR<sub>BAS</sub> in WT and PHD1<sup>-/-</sup> neurons (n = 5, p = NS). **E**, Relative change of OCR<sub>MAX</sub> and OCR<sub>ATP</sub> compared to OCR<sub>BAS</sub> (dotted line) in WT and PHD1<sup>-/-</sup> neurons (n = 3, p = NS). **F**, Glutamine oxidation measured over 2 hours in WT and

PHD1<sup>-/-</sup> neurons (n = 8, \* p < 0.05). All quantitative data are mean ± SEM. See also Figure S3 and Table S2.

Author Manuscript

Author Manuscript

Author Manuscript

Author Manuscript

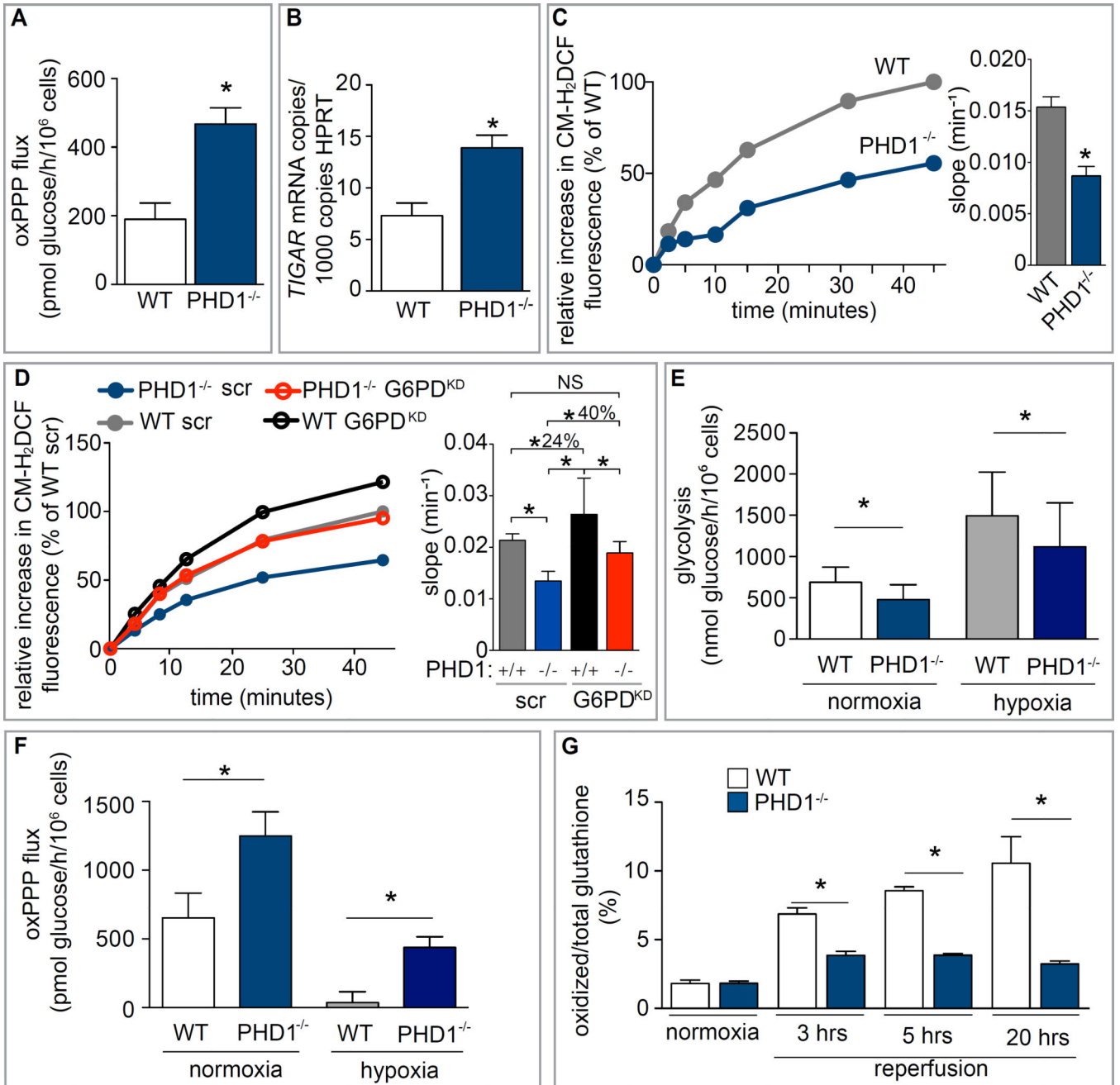


**Figure 4. Enhanced oxPPP flux in PHD1<sup>-/-</sup> neurons improves redox balance**

**A**, oxPPP flux in WT and PHD1<sup>-/-</sup> neurons (n = 4, \* p < 0.05). **B**, mTIGAR mRNA expression levels (expressed as mRNA copies/10<sup>3</sup> copies HPRT) in PHD1<sup>-/-</sup> neurons (n = 11, \* p < 0.05). **C**, Left: Increase in CM-H<sub>2</sub>DCF fluorescence (expressed as percentage of the fluorescence value in WT neurons at 45 min) after administration of H<sub>2</sub>O<sub>2</sub> to WT or PHD1<sup>-/-</sup> neuronal cultures. Right: Slope values of the curves shown in the left part, obtained by linear mixed-effect model statistics (the lower the slope, the larger the ROS scavenging capacity) (n = 3, \* p < 0.05). For reasons of clarity, only the average of the individual fluorescence values is shown without SEM, since the statistical analysis was done using the

slopes, calculated by linear mixed-effects model statistics on the individual fluorescence values (also in panel D). **D**, Left: Increase in CM-H<sub>2</sub>DCF fluorescence (expressed as percentage of the fluorescence value in control (scrambled) WT neurons at 45 min) over time after administration of H<sub>2</sub>O<sub>2</sub> to WT or PHD1<sup>-/-</sup> neurons with and without G6PD silencing (G6PD<sup>KD</sup>). Right: Slope values of the curves shown in the left part, obtained by linear mixed-effect model statistics on the individual fluorescence values (n = 3, \* p < 0.05). The percentage increase in slope value induced by G6PD<sup>KD</sup> in PHD1<sup>-/-</sup> neurons (blue *versus* red bar; 40%) is higher than in WT neurons (grey *versus* black bar; 24%). **E**, Glycolytic flux in WT and PHD1<sup>-/-</sup> neurons in normoxic and hypoxic conditions (0.1% O<sub>2</sub> for 2 hours) (n = 4, \* p < 0.05). **F**, Oxidative PPP flux in WT and PHD1<sup>-/-</sup> neurons in normoxic and hypoxic conditions (0.1% O<sub>2</sub> for 2 hours) (n = 3; \* p < 0.05). **G**, Oxidized glutathione (GSSG) levels, as percentage of the total glutathione (GSSG + GSH) levels at different time points during reperfusion in WT *versus* PHD1<sup>-/-</sup> neurons (n = 3, \* p < 0.05). All quantitative data are mean ± SEM. See also Figure S4 and Table S3.

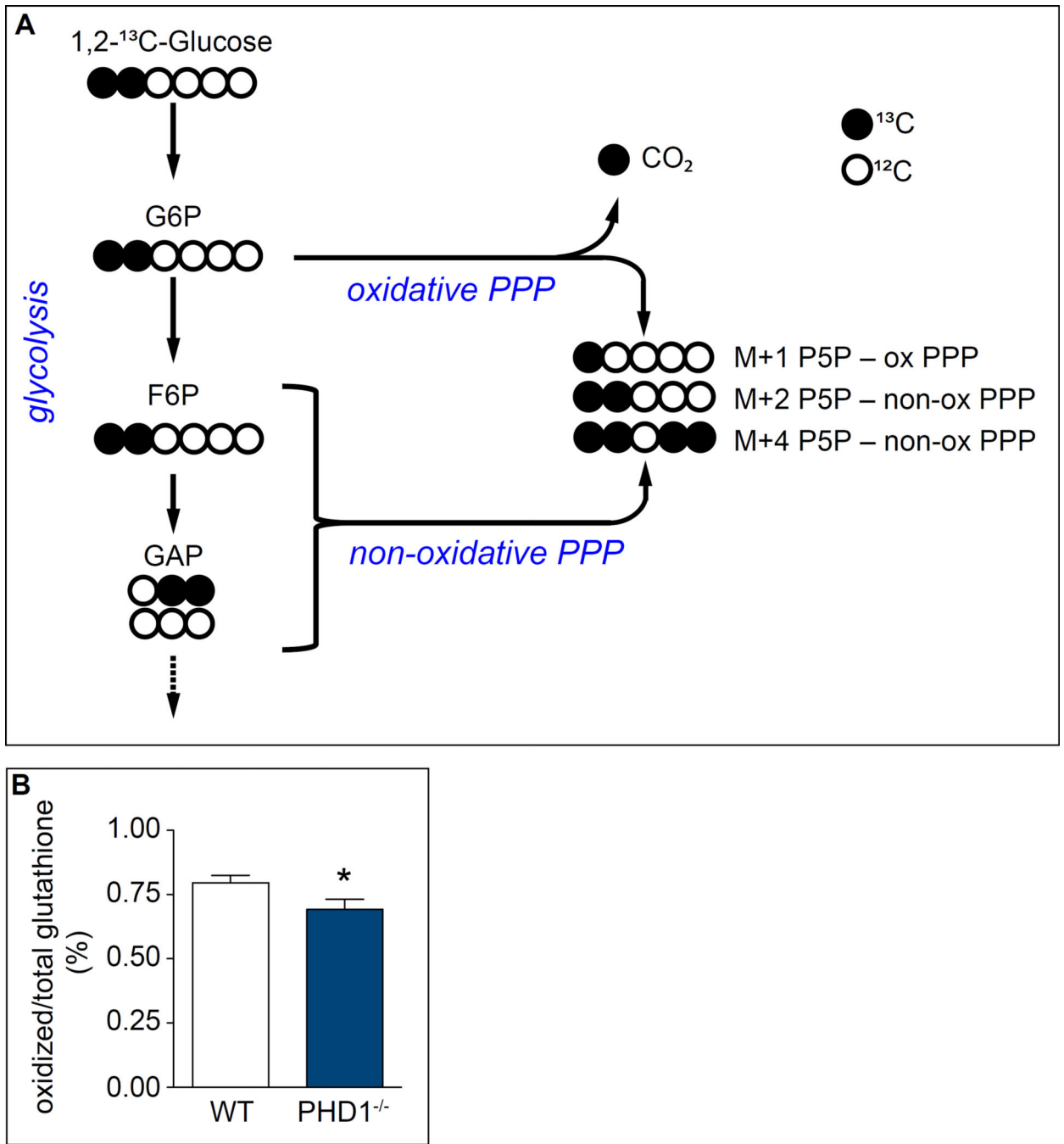


**Figure 5. PHD1 deficiency increases the oxPPP in brain and favors redox homeostasis during ischemic stress *in vivo***

**A**, Scheme depicting glycolysis and the oxidative and non-oxidative branch of the PPP, and the isotopomer distribution of 1,2-<sup>13</sup>C-glucose in the PPP. M+1 pentose-5-phosphate (P5P) can arise when glucose-6-phosphate (G6P) is converted via the oxidative PPP, while M+2 P5P can arise from the non-oxidative PPP when there is either a net or exchange flux towards P5P. F6P, fructose-6-phosphate; GAP, glyceraldehyd-3-phosphate; PPP, pentose phosphate pathway (for analysis of M+4 P5P, see methods). **B**, Levels of oxidized

glutathione (GSSG), as percentage of total glutathione (GSSG + GSH) levels in dissected brain hemispheres of WT and PHD1<sup>-/-</sup> mice after ischemic stroke (n = 7 WT mice, n = 5 PHD1<sup>-/-</sup> mice; \* p < 0.05; difference in means: -0.104 *versus* WT, 95% CI: -0.204 to -0.0045). All quantitative data are mean ± SEM.

Author Manuscript

Author Manuscript

Author Manuscript

Author Manuscript

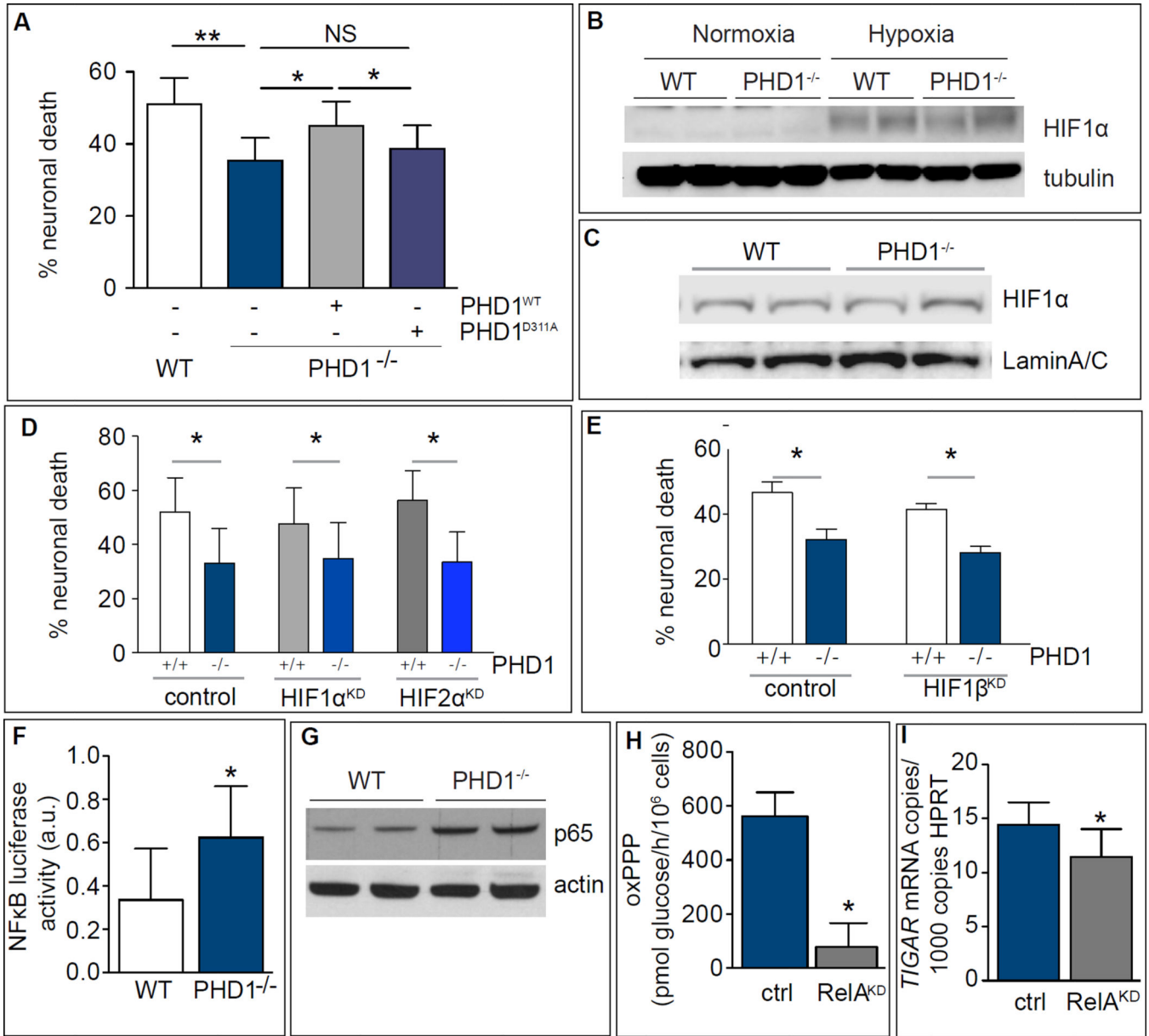


**Figure 6. Hydroxylation-dependent, HIF-independent protection against ischemia in PHD1<sup>-/-</sup> neurons via NF-κB regulated increase of oxPPP**

**A**, Neuronal cell death measured by LDH release (% of maximal LDH release) in control WT neurons, control PHD1<sup>-/-</sup> neurons, PHD1<sup>-/-</sup> neurons expressing WT PHD1 (PHD1<sup>WT</sup>), and PHD1<sup>-/-</sup> neurons expressing hydroxylation-inactive PHD1 mutant (PHD1<sup>D311A</sup>) (n = 5; \* p < 0.05). **B**, Representative western blots showing protein levels of HIF-1α in normoxic and hypoxic WT and PHD1<sup>-/-</sup> cortical neurons. Densitometric quantification of independent experiments (% of tubulin loading control): 41.2 ± 20.1% in WT and 41.9 ± 20.9% in PHD1<sup>-/-</sup> in normoxia, 129.7 ± 46.7% in WT and 122.9 ± 46.7% in PHD1<sup>-/-</sup> in hypoxia, n = 3, p = NS). **C**, Representative western blots showing protein levels of HIF-1α in WT and PHD1<sup>-/-</sup> brains. Densitometric quantification (% of lamin A/C): 58.3 ± 15.4% in WT and 57.7 ± 20.4% in PHD1<sup>-/-</sup>, n = 4, p = NS). **D**, Neuronal cell death measured by LDH release

(% of maximal LDH release) over 24 hours after oxygen-nutrient deprivation in WT and PHD1<sup>-/-</sup> neurons upon silencing of HIF-1 $\alpha$  (HIF1 $\alpha$ <sup>KD</sup>) or HIF-2 $\alpha$  (HIF2 $\alpha$ <sup>KD</sup>) (n = 3, \* p < 0.05). **E**, Neuronal cell death measured by LDH release (% of maximal LDH release) over 24 hours after oxygen-nutrient deprivation in WT and PHD1<sup>-/-</sup> neurons upon silencing of HIF-1 $\beta$  (n = 3, \* p < 0.05). **F**, NF- $\kappa$ B luciferase reporter activity in WT and PHD1<sup>-/-</sup> neurons (a.u. arbitrary units, n = 3, \* p < 0.05). **G**, Representative western blots of p65 levels in WT and PHD1<sup>-/-</sup> neurons. Densitometric quantification of independent experiments (% of loading control  $\beta$ -actin): 76.6  $\pm$  8.4% in WT and 95.9  $\pm$  8.4% in PHD1<sup>-/-</sup> neurons, n = 3, p < 0.05). **H**, oxPPP flux in PHD1<sup>-/-</sup> neurons upon silencing of RelA (RelA $\alpha$ <sup>KD</sup>) (n = 4, \* p < 0.05). **I**, TIGAR mRNA expression in PHD1<sup>-/-</sup> neurons upon silencing of RelA (RelA $\alpha$ <sup>KD</sup>) (n = 8, \* p < 0.05). All quantitative data are mean  $\pm$  SEM. See also Figure S5.

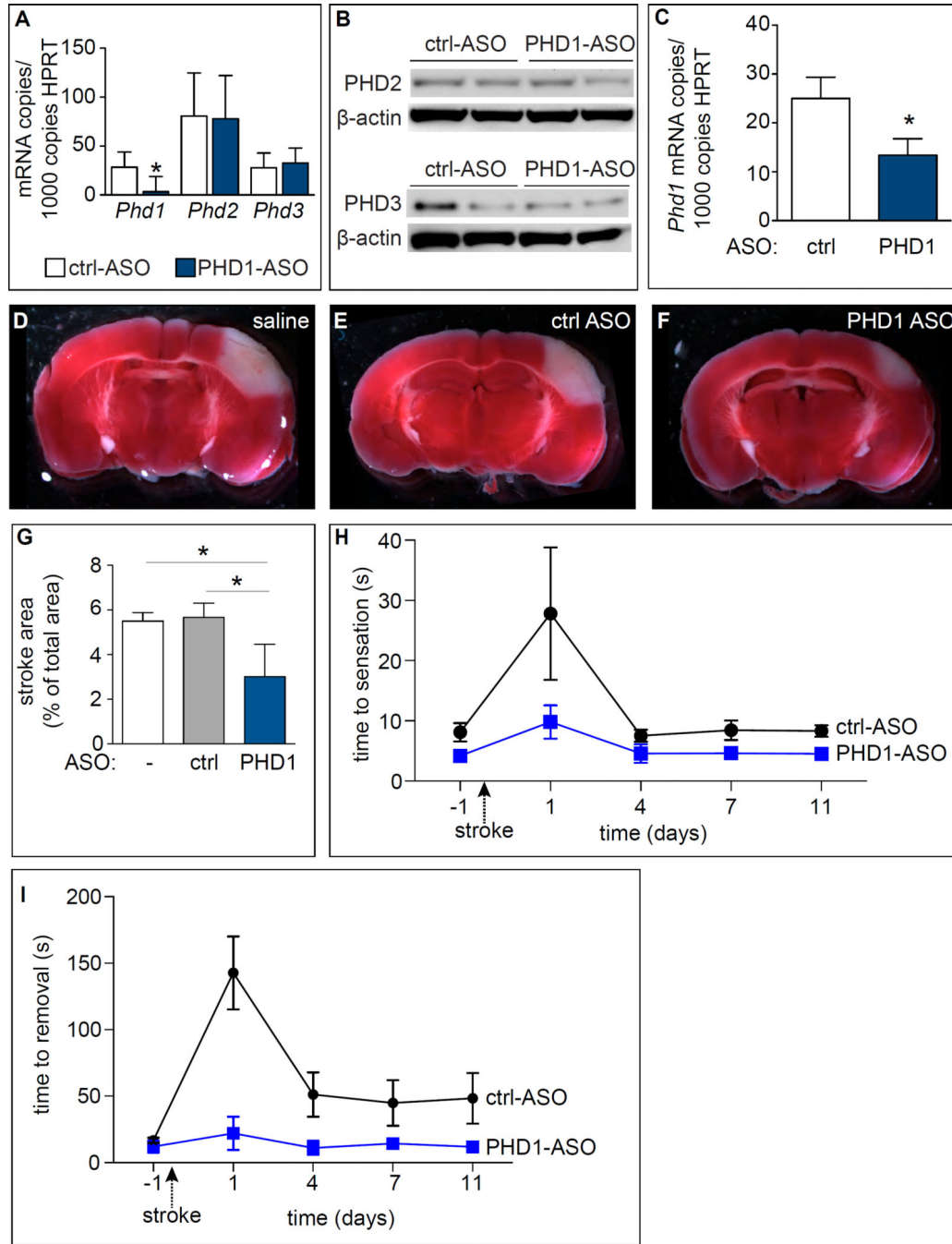


**Figure 7. Silencing of PHD1 via intracerebroventricular delivery of ASOs protects against permanent brain ischemia**

**A**, mRNA expression levels of *Phd1*, *Phd2* and *Phd3* in neuronal cultures incubated with anti-PHD1 (PHD1-ASO) and control oligonucleotides (ctrl-ASO) (0.5  $\mu$ M) for 5 days (n = 3, \* p < 0.05). **B**, Representative western blots showing protein levels of PHD2 and PHD3 in control-ASO treated and anti-PHD1 ASO treated WT neurons. Densitometric quantification of independent experiments (% of loading control  $\beta$ -actin): 72  $\pm$  17% in ctrl-ASO treated WT neurons and 64  $\pm$  17% in anti-PHD1 ASO treated WT neurons for PHD2, 28  $\pm$  15% in

ctrl-ASO treated WT neurons and  $28 \pm 13\%$  in anti-PHD1 ASO treated WT neurons for PHD3,  $n = 3$ ,  $p = \text{NS}$ . **C**, mRNA expression levels of *Phd1* in brain homogenates from control treated mice and anti-PHD1 ASO treated mice ( $n = 4$  for control treated mice,  $n = 5$  for anti-PHD1 ASO treated mice; \*  $p < 0.05$ ). **D-F** Representative brain slices after TTC staining, delineating the infarct zone as an unstained area (white), from control mice receiving saline (D), an ASO against human huntingtin (E) or an anti-PHD1 directed ASO (F), 24 hours after pMCAO. **G**, Quantification of the stroke area as percentage of the total bihemispheric area ( $n = 11$  for the saline group,  $n = 5$  for the control ASO group,  $n = 9$  for the anti-PHD1 ASO group, \*  $p < 0.05$ ; difference in means:  $-2.49$ , 95% CI:  $-3.76$  to  $-1.22$  for PHD1 ASO *versus* saline; and difference in means:  $-2.66$ , 95% CI:  $-4.40$  to  $-0.92$  for PHD1 ASO *versus* control ASO). **H,I**, Measurements of the adhesive tape removal test at 1 day before and at day 1, 4, 7 and 11 post-stroke. Average time needed before control-ASO treated (gray,  $n = 9$ ) and anti-PHD1 ASO treated (blue,  $n = 7$ ) mice sensed the presence of the tape (H) ( $p = 0.057$ , repeated-measure ANOVA). Average time needed before the mice successfully removed the tape (I) ( $n = 9$  for control-ASO treated mice,  $n = 7$  for anti-PHD1 ASO mice,  $p < 0.05$ , repeated-measure ANOVA). All quantitative data are mean  $\pm$  SEM.